An investigation into shrinkage and collapse behavior of *Eucalyptus grandis* and *Eucalyptus grandis x urophylla* wood

by

Nkosinamandla Artwel Sizwe Gonya

Thesis presented in partial fulfilment of the requirements for the degree of
Master of Science

at

Stellenbosch University
Forestry and Wood Science, Faculty of AgriSciences

Supervisor: Dr Brand Wessels

March 2020

Declaration

By submitting this thesis electronically, I declare that the entirety of the work contained therein is my own, original work, that I am the sole author thereof (save to the extent explicitly otherwise stated), that reproduction and publication thereof by Stellenbosch University will not infringe any third-party rights and that I have not previously in its entirety or in part submitted it for obtaining any qualification.

Date: March 2020

Summary

Only 1 % of land is used for forestry in South Africa and the country might experience a shortage of structural softwood sawn timber in the near future. Despite this, South Africa actually produces more *Eucalyptus* logs than the local processing industry can process, hence end up exporting large volumes of *Eucalyptus* chips to foreign countries. Additionally, on average, the annual increment of South African *E. grandis* is almost twice that of South African *Pinus* species. Recently, the green processing of *Eucalyptus* lumber into engineered wood products has been investigated. However, the variation of dimensional changes during the drying process due to shrinkage and collapse make the efficient processing of *Eucalyptus* lumber a challenge. A better understanding of the shrinkage and collapse behaviour of *Eucalyptus grandis* and *Eucalyptus grandis X urophylla* might enable improved lumber separation and processing.

The objectives of the study were to profile the variations of (1) collapse and (2) shrinkage (a) radially and (b) along the height of trees and to explore the *relationships* they have with basic physical properties of the tree. The hypothesis was that the non-uniform dimensional changes found in the end products of *Eucalyptus grandis* are due to these variations. Seventy trees of *Eucalyptus grandis* and *Eucalyptus grandis X urophylla* were collected from Tzaneen, Limpopo, South Africa. The trees were selected based on age, genetic improvement, as well as an additional splitting trial: 10x trees young (8 yrs) and genetically improved, 10x trees young (7 yrs) and genetically unimproved, 10x trees mature (13 yrs) and genetically improved, 10x trees mature (13 yrs) and genetically unimproved, 20x trees from a splitting trial (17 yrs) and an older trial (24 yrs). All trees were *E. grandis* except the mature groups which were *E. grandis X urophylla.* Disks that were later cut into wedges were removed from four heights (1.3 m, 6.4 m, 11.46 m, and 16.52m) from each tree. Two logs of 4.2 m were removed from two heights, processed into boards, and kiln dried. On the boards collapse was visually assessed and shrinkage measurements were taken before and after drying. On the wedge samples shrinkage, collapse, density, moisture content, permeability, extractives contents and heartwood/sapwood ratio were measured. All the samples and measurements were taken so that they give the radial variation between centre (pith), transition zone and outer wood (sapwood).

An important finding in this study was that the properties measured on small wedge samples differed significantly from what was observed on sawn boards. This was true for both collapse and shrinkage - the properties on which this study focussed.

On boards, collapse varied depending on group, log position and the radial position of the boards. The radial position of the boards had a highly significant effect on board collapse, with

collapse generally decreasing from pith to bark. There were first order interactions between all the factors and board collapse behaviour was not consistent throughout groups and log positions. In terms of the causal factors, there were weak but significant correlations between collapse and extractives content, density, and permeability (although these results should be viewed with caution since it was obtained from the small wedge samples). A very interesting result is the weak correlation between radial and tangential collapse on small wedge samples showing the clear directional nature of collapse.

On boards, shrinkage varied depending on group, log position and the radial position of the boards. Shrinkage in the thickness direction was higher in the centre boards and decreased towards the outer boards. This was due to the effect of collapse on the thickness direction as collapse is very size sensitive and no matter the direction (radial or tangential) the wider side experienced the most collapse. In the width direction, the shrinkage followed the normal pattern increasing from centre boards towards the outer boards. The width direction shrinkage had almost similar trends with the results found on wedges in both directions (radial and tangential).

Twist, bow and cup also varied significantly radially and along the height. However, the magnitude of these was generally far better than the requirements of national standards. Bow had a similar trend as shrinkage in the width direction. The trends for twist and cup were not consistent.

Some of the results obtained from small disk samples were inconclusive and contradicted what was observed in boards. It is recommended that future studies focus on obtaining a better understanding on the effect of specimen size. Although trends observed from the small samples were interesting, the practical significance is limited if the results cannot be related to observations in industrial size boards.

Opsomming

Slegs 1% van die landarea in Suid-Afrika word vir bosbou gebruik, en die land sal moontlik binne die nabye toekoms 'n tekort aan strukturele sagtehout hê. Desondanks produseer Suid-Afrika in werklikheid meer *Eucalyptus*-stompe as wat die plaaslike verwerkingsbedryf kan verwerk, en sodoende word daar groot hoeveelhede *Eucalyptus*-spaanders na die buiteland uitgevoer. Daarbenewens is die jaarlikse groei van Suid-Afrikaanse *E. grandis* gemiddeld byna twee keer meer as die Suid-Afrikaanse *Pinus*-spesies. Onlangs is die groenbewerking van *Eucalyptus*-hout in houtprodukte ondersoek. Die variasie van dimensionele veranderinge tydens die droogproses as gevolg van inkrimping en ineenstorting maak die doeltreffende verwerking van *Eucalyptus*-hout egter 'n uitdaging. 'n Beter begrip van die krimp- en ineenstortingsgedrag van *Eucalyptus grandis* en *Eucalyptus grandis X urophylla* kan verbeterde skeiding en verwerking van hout moontlik maak.

Die doelwitte van die studie was om die variasies van (1) ineenstorting en (2) inkrimping (a) radiaal en (b) langs die hoogte van bome te beskryf en om die verwantskappe wat hulle het met die basiese fisiese eienskappe van die boom te ondersoek. Die hipotese was dat die nie-eenvormige dimensionele veranderinge in die eindprodukte van *Eucalyptus grandis* te wyte was aan hierdie variasies. Sewentig bome van *Eucalyptus grandis* en *Eucalyptus grandis X urophylla* is van Tzaneen, Limpopo, Suid-Afrika versamel. Die bome is geselekteer op grond van ouderdom, genetiese verbetering, sowel as 'n addisionele splitsingsproewe: 10x bome jonk (8 jaar) en geneties verbeter, 10x bome jonk (7 jaar) en geneties onverbeterd, 10x bome volwasse (13 jaar) en geneties verbeter, 10x bome volwasse (13 jaar) en geneties onverbeterd, 20x bome vanaf 'n splitsingsproef (17 jaar) en 'n ouer proef (24 jaar). Al die bome was *E. grandis*, behalwe die volwasse groepe wat *E. grandis X urophylla* was. Diskette wat later in wiggies gesny is, is van vier hoogtes (1,3 m, 6,4 m, 11,46 m en 16,52 m) van elke boom verwyder. Twee houtblokke van 4,2 m is van twee hoogtes verwyder, in planke verwerk en oond gedroog. Op die planke is ineenstorting visueel beoordeel en krimpmetings is voor en na droging gedoen. Op die wigmonsters is krimping, ineenstorting, digtheid, voginhoud, deurdringbaarheid, inhoud van uittreksels en hart- / saphoutverhouding gemeet. Al die monsters en metings is geneem sodat dit die radiale variasie tussen middel (“pith”), oorgangsone en spinthout (“sapwood”) gee.

'n Belangrike bevinding in hierdie studie was dat die eienskappe wat op klein wigmonsters gemeet is, beduidend verskil van wat op saagplanke waargeneem is. Dit geld vir beide ineenstorting en krimping - die eienskappe waarop hierdie studie gefokus het.

Op die planke het die ineenstorting verskil, afhangende van die groep, stomp-posisie en die radiale posisie van die planke. Die radiale posisie van die planke het 'n baie belangrike uitwerking op die ineenstorting van die hout gehad, en die ineenstorting het meestal van pit tot bas afgeneem. Daar was eerste orde interaksies tussen al die faktore, en die gedrag van die direksie-ineenstorting was nie konsekwent in groepe en stompposisies nie. Wat die oorsaaklike faktore betref, was daar swak, maar beduidende korrelasies tussen ineenstorting en ekstraksie-inhoud, digtheid en deurlaatbaarheid (alhoewel hierdie resultate met omsigtigheid beskou moet word, aangesien dit uit die klein wigmonsters verkry is). 'n Baie interessante resultaat is die swak korrelasie tussen radiale en tangensiële ineenstorting op klein wigmonsters wat die duidelike rigtingverwante aard van ineenstorting toon.

Afhangend van groep, stompposisie en die radiale posisie van die planke het krimping gewissel. Krimping in die dikterigting was hoër in die middelborde en neem af na die buitenste planke. Dit was te danke aan die effek van ineenstorting op die dikterigting, aangesien ineenstorting baie sensitief is vir die grootte en dit maak nie saak die rigting (radiaal of tangensiëel) wat die breër kant die meeste ineenstorting ervaar het nie. In die breedterigting volg die inkrimping die normale patroon wat van die middelborde na die buitenste planke toeneem. Die inkrimping van die breedterigting het byna soortgelyke neigings gehad met die resultate wat op albei rigtings se wiggies gevind is (radiaal en raaklynig).

Draai, boog en koptrek het ook aansienlik radiaal en langs die hoogte gevarieer. Die omvang hiervan was egter oor die algemeen baie beter as die vereistes van nasionale standaarde. Boog het 'n soortgelyke neiging gehad as krimp in die breedterigting. Die neigings vir draai en koptrek was nie konsekwent nie.

Sommige van die resultate wat op klein skyfmonsters verkry is, was onoortuigend en weerspreek dit wat in planke gesien is. Dit word aanbeveel dat toekomstige studies fokus op die verkryging van 'n beter begrip van die grootte van die monster. Alhoewel tendense wat by die klein monsters waargeneem is, interessant was, is die praktiese belang daarvan beperk as die resultate nie verband hou met waarnemings in industriële grootte planke nie.

This thesis is dedicated to

Myself

Acknowledgements

I wish to express my sincere gratitude and appreciation to the following persons and institutions:

- Dr. Brand Wessels for his supervision of this study, guidance and support he offered throughout this project.

- A sincere thank you to the Department of Forestry and Wood Science especially Justin Erasmus for his help with the statistical analysis.

- Thanks to the Hans Merensky Foundation for providing funding for this project.

- The Northern Timbers sawmill for providing the samples for the study.

- My greatest thanks to my family and friends for the constant support throughout this process.

Table of Contents

List of figures

List of tables

Abbreviations and Acronyms

YI	Young Improved
YU	Young Unimproved
MI	Mature Improved
MU	Mature Unimproved
EX	Splitting Trial
OL	Old Group
EP	Elite Population
MC	Moisture Content
H/S ratio	Heartwood/Sapwood ratio
FSP	Fiber Saturation Point
MFA	Micro Fibril Angle
ANOVA	Analysis of Variance

Chapter 1: Introduction

1.1 Background

Only 1% of land is used for forestry in South Africa and according to Crafford and Wessels (2016) South Africa is a timber-scarce country which will experience a shortage of structural softwood timber in the near future. According to Chamberlain et al. (2005) and Crafford and Wessels (2016), South Africa produces more *Eucalyptus* logs than the processing industry can process, hence end up exporting tons of *Eucalyptus* as chips for pulp production to foreign countries. Additionally, softwood pine plantations are often replaced with hardwood eucalypt plantations. Crickmay and Associates (2005) stated that the mean annual increment of South African *Eucalyptus grandis* is almost twice that of South African Pine (*24.6* $m^3.ha^{-1}.y^{-1}$ *and 14.6* $m^3 .ha^{-1}.y^{-1}$ respectively). *Eucalyptus* timber is rarely processed into structural timber due to its shortcomings such as dimensional instability, splitting, checking, collapse, and brittle heart (Jacobs 1955; Malan 1984; Malan 1993; Vermaas and Bariska 1994; Yang and Waugh 2001; Malan 2003; Crafford and Wessels 2016). Shrinkage and collapse occur because of wood losing water and dimensions of wood changing resulting in a variety of problems in the processing of eucalypt timber. Recently, the green processing of *Eucalyptus* lumber into engineered wood products have been investigated. However, the variation of dimensional changes during the drying process due to shrinkage and collapse make the efficient processing of *Eucalyptus* lumber a challenge. A better understanding of the shrinkage and collapse behaviour of *Eucalyptus grandis* and *Eucalyptus grandis X urophylla* might enable improved lumber separation and processing. In order to understand these problems better and to develop strategies to deal with them, a better understanding is required of the within -and between tree variation in shrinkage and collapse. This study, therefore, evaluated shrinkage and collapse of *E. grandis* and *E. grandis x E. urophylla* wood and the properties that affect them. The gradients of the above mentioned were evaluated (how they change from pith to bark and with the height of the tree) as well as their relationships with basic wood properties such as density, extractives content, and moisture content (MC).

1.2 Problem Statement

Ash type eucalypts (with densities less than 500 kg/m^3) are known to be prone to collapse and excessive and varying shrinkage. This dimensional instability leads to an uneven surface of the final product after drying, resulting in a lot of wastage during the planing of the products. Understanding the variation in shrinkage and drying could help with solutions for this problem. One option may be to group boards with similar shrinkage and collapse

tendencies together and process them differently (i.e. higher planing allowance for high shrinkage/collapse boards).

1.3 Objectives

The objectives of the study were:

- To determine the shrinkage and collapse variation (radially and by height) of *E. grandis* and *E. grandis x urophylla* wood from trees of different ages and sites.
- To investigate the basic wood and tree properties that may influence shrinkage and collapse and determine the relationships between them.

Chapter 2: Literature Review

2.1 Shrinkage

Shrinkage or swelling of wood is the change in the dimensions of the wood (increase or decrease) due to moisture fluctuations below the fibre saturation point (FSP). The moisture fluctuations above FSP do not result in significant changes in the dimensions (Tsoumis, 1991). Wood loses water to equilibrate its moisture content to its surrounding environment if the surrounding environment is dry, and also takes up water when the surrounding environment is humid; hence shrink and swell. The shrinking and swelling of wood is associated with moisture content but there are a lot of other factors that influence this process (see *figure 2-1*) for the relationship between moisture content and shrinkage. Furthermore, wood is anisotropic; implying that shrinkage magnitude is direction dependent (Tsoumis 1991; Wang et al. 2008). Hence, shrinkage properties in the three dimensions (radial; longitudinal; and tangential) are not similar. Shrinkage and collapse have a similar effect on wood as they both reduce its dimensions and hence, a distinction between collapse-free shrinkage and shrinkage including collapse is important.

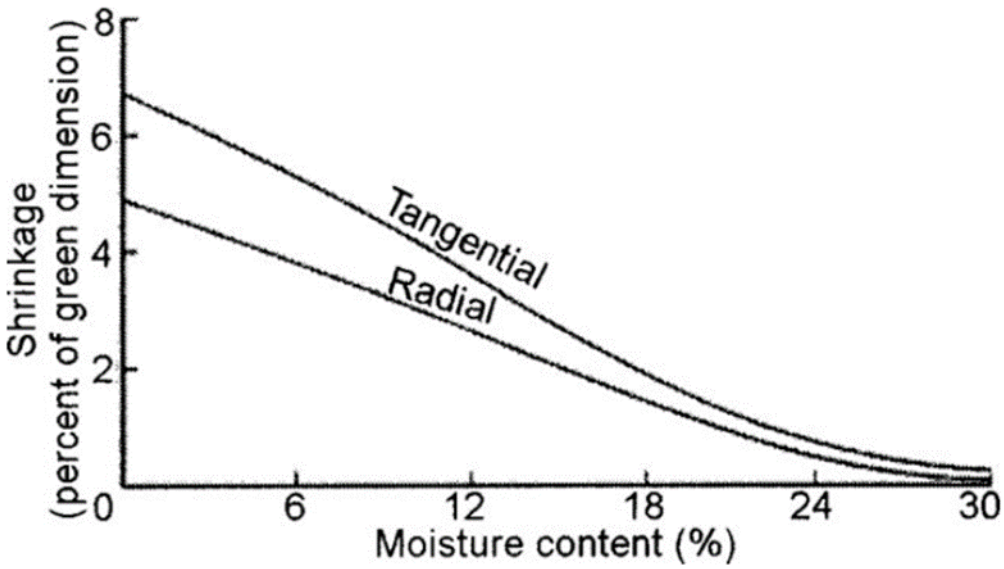

Figure 2- 1: The relationship between shrinkage and moisture content (Carl and Wiedenhoeft 2009).

2.2 Collapse

Most species of the genus *Eucalyptus* are prone to collapse (Sun et al. 2013) and experience collapse related internal/surface checking. As a result, it is recommended that boards should be reconditioned at a mean moisture of between 15% and 20%. (Kauman 2002; Wu et al. 2005; 2006; Blackmore et al. 2007; and Yang and Liu 2018) described collapse as an abnormal shrinkage occurring in woods of certain tree species during the drying process. Further, (Blackmore et al. 2007; Ananías et al. 2014; Akbari et al. 2015; Yang and Liu 2018) stated that collapse occurs above the fibre saturation point and it is commonly explained by capillary tension (liquid tension). Bateson (1946) reported collapse or wash-boarding as a result of wood shrinking more in certain growth rings than others possibly due to variation in density. In addition, Bariska et al. (1992) reported that collapse occurs immediately after felling and that collapse occurs in living trees as well. See *figure 2-1* (A) showing the collapsed cells. Research has been done on preventing or overcoming collapse and collapse related internal checking in low to medium density eucalypts, particularly the 'Ash' type eucalypts (Wu et al. 2006; Blackmore et al. 2007). Furthermore (Illic 1999; Blackmore et al. 2007) distinguished collapse prone boards as those with a basic density of less than 500 kg/m^3. Bhat et al. (1990) reported that 3-year old *Eucalyptus grandis* have a mean density of 495 kg/m^3 and no significant increase from 3 years to 9 years.

Collapsed cells can be recovered especially during the reconditioning of the wood at the end of the drying process (see *figure 2-2 B*). From the distinguishing factor used by Blakemore et al. (2007), woods of low density are more prone to collapse and collapse related internal checking. As collapse is explained by capillary tension, (Ananías et al. 2014 and Yang et al. 2018) stated that low permeability of the transition wood of *Eucalyptus nitens* can cause high capillary forces as a result of higher tension, hence higher incidences of collapse were reported for above-mentioned eucalypt species. It is necessary for the cell lumens to be saturated for collapse to take place. Furthermore; Yang and Liu (2018) explained that there are a number of contributing factors to collapse, as such that it can happen that the wood is impermeable but is of high density and the cell walls can withstand the capillary forces hence, one criterion overcomes the other. Also, if the wood has air pockets in its cells they can move into the spaces where water moves out and counter the capilary forces (Yang et al., 2018). During drying, collapse is a function of the temperature, with high temperatures causing more collapse because of higher moisture content gradients. The most important requirement for collapse is the presence of water in the cell lumens (high initial moisture content) (Yang et al. 2003;2018).

Bariska (1992) reported that collapse is the result of capillary tension due to movement of water out of the wood or between cells in the wood. The same tension results if the water intake

by the roots is less than the transpiration in the tree crown of a living tree, and a large hydrostatic gradient might consequently build up in the stem. This is usually the case when there is not enough water in the soil especially during drought or frost conditions. As a result, collapse can be experienced by living trees due to the low cross grain tensional strength in green wood.

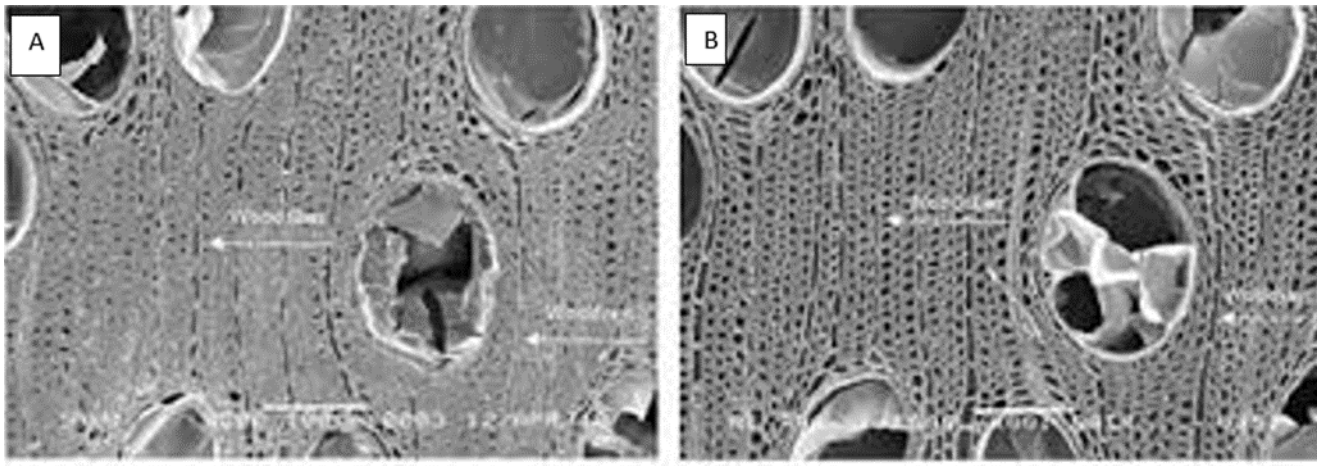

Figure 2- 1: Picture showing (A) collapsed cells and (B) recovered cells under microscope (Yang and Liu 2018)

2.3 Properties that influence shrinkage and collapse

2.3.1 Density

Density is often considered the most important property of wood as other properties, both mechanical and physical properties, can be predicted using density. (Washusen et al. 2001; Kord et al. 2010; Hein et al. 2013; Schulgasser et al. 2015) have reported on the density and its different relationships including shrinkage. Density has a positive relationship with shrinkage. Studies by (Washusen et al. 2001; Schulgasser and Witztum 2015) have reported high densities to be associated with high shrinkage. However, Kord et al. (2010) have reported density to have the above-mentioned relationship with only radial and tangential shrinkage, as the longitudinal shrinkage does not necessarily increase with increasing density. According to Hein et al. (2013) high densities does not necessarily correlate to high microfibril angle (MFA) and the longitudinal shrinkage correlates better to the MFA than density. Furthermore, Kord et al. (2010) reported the density of *Populous euramericana* to decrease with tree height. As discussed by Lukášek et al. (2012) there is a strong relationship between wood density and tangential and radial shrinkage. Hence radial and tangential shrinkage along the axis can be predicted with density as it decreases with the tree height as well.

Some studies have found that a weak positive relationship exist between density and longitudinal shrinkage. (Kord et al. 2010 and Lukášek et al. 2012) reported that some wood species' shrinkage tends to decrease as wood density increases. According to Kord et al.

(2010) longitudinal shrinkage decreases from pith to bark as opposed to the increasing density. However, the density decreases with the tree height and so did the longitudinal shrinkage of *Populous euramericana.* Washusen et al. (2001) reported a strong linear relationship between microfibril angle and density. According to Kord et al. (2010) dense wood result from thick cell walls and low microfibril angles and produces minimal longitudinal shrinkage (Schulgasser and Witztum, 2015) and increased radial and tangential shrinkages. The microfibril angle has a major effect on wood stiffness and on drying shrinkage of wood according to Hein et al. (2013) and Schulgasser et al. (2015). Stiff wood is also of high density and low microfibril angle, hence these three wood properties would better predict the longitudinal shrinkage of wood.

2.3.2 Microfibril Angle

Microfibril angle is the angle at which the cellulose is oriented from the cell axis (Yamashita et al. 2009). At microscopic level wood cells walls are made of the middle lamella, which acts as a joint between cells. The cell wall is made of three layers S_1, S_2 and S_3, the cellulose microfibrils in the primary cell wall and S_3 are transversely oriented. The S_2 layer has microfibrils oriented at an angle from the cell axis varying between 10° to 30°. The S_2 is the thicker layer of the three and dominates the physical properties of the cell wall (Bossu et al. 2016). When the MFA is small the high shrinkage is observed transversely, while with an increasing MFA the longitudinal shrinkage increases in a non-linear manner (Yamashita et al. 2009; Hein et al. 2013). Bossu et al. (2016) suggested that transverse shrinkage is mostly influenced by basic density, while for longitudinal shrinkage the cell fibre orientation prevails. Yamasita et al. (2009; 2009) reported that longitudinal shrinkage was higher in juvenile wood and compression wood in which microfibril angle is also high. Hein et al. (2016) reported weak correlations between MFA and shrinkage (radial and tangential) with r^2 values of -0.24 and -0.33 respectively in *Eucalyptus* wood, the reason for the weak correlations being the narrow range of the MFA variation. The dimensions of cellulose microfibrils does not necessarily change but rather the matrix (orientation) of the cell wall changes. Microfibrils act as to restrain the matrix from shrinkage (Hein et al. 2016). Yamashita et al. (2009) reported a trend whereby MFA decreases towards the bark for *Cryptomeria japonica* and density is known to increase towards the bark.

2.3.3 Hygroscopicity

Tsoumis (1991) explained hygroscopicity as a property of wood related to the attraction of water from the surrounding atmosphere and holding it in the form of liquid or water vapour. The importance of hygroscopicity can be explained by the effect that moisture has in wood and on other wood properties such as shrinkage and density. Washusen et al. (2001) determined the relationship between wood density and shrinkage as they both are heavily affected by the moisture content of wood. Water in wood is either stored as bound water (found in cell walls) or free water (found in cell cavities). Shrinkage results from the process whereby water in cell walls

(bound water) evaporates resulting in dimensional changes below FSP. Collapse below FSP occurs as the non-linear part of shrinkage. These processes happen as a result of water evaporating from the surface of the wood, creating a moisture gradient (the gradient can be steeper with high drying temperatures). Then the free water in the cell lumens moves from cell to cell until it reaches the exposed surface where it evaporates. Once all the free water has escaped, the FSP is reached where the only water in wood is bound water (in the cell wall) - at this point only collapse takes place no shrinkage. As soon as the wood starts losing the bound water below FSP; then the wood starts to shrink (Tsoumis, 1991).

2.3.4 Moisture content

Various studies have reported on the differences in moisture content of wood disks from pith to bark. Tsoumis (1991) reported that there is very high difference between the moisture content (MC) in heartwood and sapwood of softwoods whilst the difference is not that high with hardwoods. The difference in moisture content of the heartwood and sapwood can be attributed to the bulking amount of water-soluble extractives content in the cell walls of the heartwood, which reduces the space available for adsorption (Choong, undated). Further, more studies have been done on the variation of the shrinkage in the stem of the log and relationships between primary factors that affect shrinkage and shrinkage itself (Wiedenbeck et al. 1989; Washusen et al. 2001; Lukasek et al. 2012; and Schulgasser et al. 2015). The factors evaluated include but not are limited to density, extractives content and microfibril angle. The differences between sapwood and heartwood, mature wood and juvenile wood and early wood and late wood also influence the shrinkage of wood.

2.3.5 Radial differences across the tree disk

The effect of density has been explained by the amount of cell wall (cell wall thickness) especially in the S_2 layer (Bossu et al. 2016). Washusen et al. (2001), Kord et al. (2010), and Derome et al. (2011) reported that wood with higher densities have thick cell walls. Furthermore, high density wood absorbs more moisture in the cell wall as there is more material to take up water and availability of sorption areas is more, hence swell more and shrinks more. Yamashita et a. (2009; 2009) suggested that the amount of shrinkage is proportional to the amount of cell wall material or moisture loss from the cell wall hence, shrinkage increase with increasing density. That also explains the difference in early wood and late wood shrinkage. Late wood shrinks more because of higher density than that of early wood (Schulgasser and Witztum, 2015). The increase of moisture content from pith to bark as reported by some (Tsoumis 1991; Kord et al. 2010) can be explained by the fact that juvenile wood (core wood) is known to be of low density, while the mature (outer wood) is known to be of higher density. Bao et al. (2001) and Yamashita et al. (2009) reported that juvenile wood has a large microfibril angle and

significant shorter tracheids/fibers than mature wood. Hence radial shrinkage and tangential shrinkage increases from pith to bark and according to Washusen et al. (2001) shrinkage of the sapwood is significantly greater than that of heartwood of *Eucalyptus globulus*. In contrast Ananías et al. (2014) found a different trend for *Eucalyptus nitens* where it was reported that for some trees the density increased from pith to the transition wood and then decreased from transition wood to the outer wood. Shrinkage and collapse of this tree species followed the same trend as density with the peak values at the transition zone of the tree disk. Furthermore, they reported the moisture content to be decreasing from pith to bark; hence no specific correlation could be noted with density and either shrinkage or collapse.

2.3.6 Extractives contents

Extractive content has been studied for its effect on the shrinkage of wood and may better explain the significant difference between sapwood and heartwood than other properties (Washusen et al. 2001; Bossu et al., 2020)). The core wood is made up of juvenile wood with mostly undesirable properties. It is composed of dead cells and its chemical composition is different from that of sapwood (Bao et al., 2001). The chemical composition of the core wood (heartwood) is in some cases advantageous as it gives the natural durability and protection against wood degraders such as termites without the need for treatment (Sharma et al., 2015). In some species it is easy to separate heartwood from sapwood due to the darker colour of the heartwood as a result of extractives contents deposition. On the other hand, the sapwood consists of live cells and the cambium that transports water from the roots through the stem to the leaves. Hence it is more susceptible to the wood degraders such as termites than the heartwood. Washusen et al. (2001) concluded that both density and extractive contents influence shrinkage of wood. (Bossu et al., 2020) found that the volume shrinkage of un-extracted wood was greater in the sapwood than in the heartwood, while the extracted wood had an increased shrinkage in the heartwood. He and Tsoumis (1991) further found that more extractives were removed from the heartwood and that there exists an inverse relationship between extractives contents and shrinkage. This might be the result of the fact that extractives occupy the space and reduces the sorption areas for water and further, water evaporates at 100°C while extractives remain in the wood at that temperature. This also explains the increasing shrinkage from pith to bark as the sapwood mainly consists of water, while the heartwood consists of the extractives with a different chemical composition than that of sapwood (Bao et al. 2001). According to Oliver (1991) in Priadi (2001) lignin can stiffen the cells and reduce the collapse occurrence in mature wood.

2.3.7 Permeability

Permeability is the ability of a material to allow the movement of a substance through it, as for wood this is the ability to allow substances such as water/air to move through its pores (vessels, rays and tracheid's). This ability depends on the size of the openings of the pores and whether they are open or closed. The deposition of extractives in the heartwood reduces the pit sizes by partially closing the openings hence, the heartwood is highly impermeable. Wood with high permeability is easy to impregnate with substances such as chemicals for preservative treatment. Most species' heartwood are impermeable while sapwood are highly permeable. Mugabi (2007) stated that samples of *Eucalyptus regnans* consisting of sapwood collapsed less than the ones consisting of heartwood mainly due to permeability. In another study by Ilic (1999) it was stated that during drying collapse occurs as a result of the removal of water from highly impermeable wood fibres (cells) which become distorted as a result of high tensile forces generated in the cell lumens. Mugabi (2007) suggested that woods which are air permeable are also less prone to collapse and that may be why collapse does not occur at the edge of the wood or the sapwood. Further, Thomas and Erickson (undated) did some work on the relationship between collapse, honeycomb and liquid permeability of red cedar. They only examined collapse visually with evidence like wash-boarding and they concluded that the wood that had evidence of collapse was also less permeable. Furthermore, if the wood is permeable, air flows through it and forms air pockets which inhibit the capillary tension during the water movement by moving into spaces that were occupied by water (Priadi 2001; Yang and Liu 2018).

2.3.8 Structure and chemical composition of wood

Lignin has a large effect on the radial shrinkage of wood as lignin is found in the middle lamella and when removed e.g by lignin consuming wood degraders, the spaces that were occupied by lignin are then occupied by water - hence more shrinkage is observed (Nguyen et al. 2018; Jakes et al. 2019). Presence of rays also restrain the radial shrinkage. Furthermore; Barkas (1941) did some work verifying the effect of rays on the radial shrinkage and in fact found that rays do inhibit radial shrinkage and account for the anisotropic shrinkage. The same author explained that the wood consists of hollow cells (fibres) with the majority lying parallel to the grain (longitudinal direction) and give the wood its characteristic strength along the grain. He further explained that few cells (rays) lie in the radial direction, hence providing characteristic strength of wood in a radial direction. While none of the cells lie in a transverse direction and as a result wood shrinks more in the tangential direction, followed by radial and very little in longitudinal direction. According to Hillis and Brown (1984) variation in the quality of wood depends on the variations at cellular level, in the chemical composition, ultra-structural and microscopic characters of the wood; hence the difference in shrinkage of various species is structure dependent.

Chapter 3: Materials and Methods

3.1 Materials

The materials used in this study were collected from Merensky Timber plantations in Tzaneen, Limpopo, South Africa. Seventy (70) trees of *Eucalyptus grandis* and *Eucalyptus grandis X Eucalyptus urophylla* from 5 compartments were harvested for sampling (see *Table 3-1*). The compartments and their locations can be seen in *table 3-1 and figure 3-1*. The sampled trees comprised of 10 old trees (different seedstock); 20 improved trees or elite population young and matured; 20 unimproved trees young and matured; and 20 trees from a splitting trial for comparison as can be seen in *table 3-1* below. The young, unimproved group (YU) on compartment N18 was 7-year old *E. grandis X urophylla* clonal trees that was not selected for improved splitting and other properties. The young, improved group (YI) on compartment F5 was 8-year old *E. grandis* that was selected for improved splitting and other properties (elite population). The splitting trial group (EX) on compartment A13a was 17-year old *E. grandis* that was planted to compare different treatments on splitting (high/low). The mature, improved group (MI) on compartment N21 was 13-year old *E.grandis* that was selected for improved splitting and other properties. The mature, unimproved group (MU) on compartment N21 was 13-year old *E.grandis X E. urophylla* clonal trees that was not selected for improved splitting and other properties. The old group (OL) on compartment G2a was 24-year old *E. grandis* that was from a different seed stock but was included in the study to explore age as a factor. The grouping was done in such a way that it allows for the comparison between the elite population and the unimproved population, and the age effect. The north side was marked on every tree before felling (*see figure 3-2 B*). Before felling the trees, cores were taken out, resistograph was done and holes were drilled on the first log 2 meters apart for strain measurements for another study. The complete sampling plan can be seen in *figure 3-3*. Four billets of 0.15 m were taken from four different heights (1.3 m, 6.4 m, 11.46 m, and 16.52m) on each tree. The north side was marked on each sample and the top and bottom sides as well (see *figure 3-2 A*), the number (23) is the tree number, first letter (A, B, C or D) specifies the height and the last letter (B or T) specifies the side of the sample i.e bottom or top. Immediately after felling the billets were covered and tightly taped with black plastic bags to avoid moisture loss. The billets were further cut in half and then further cut into samples needed for each test as seen in the sampling plan (see figure 3-3). Boards (4.2 m long) from the first 2 logs were also evaluated for shrinkage, collapse, bow, twist and cup.

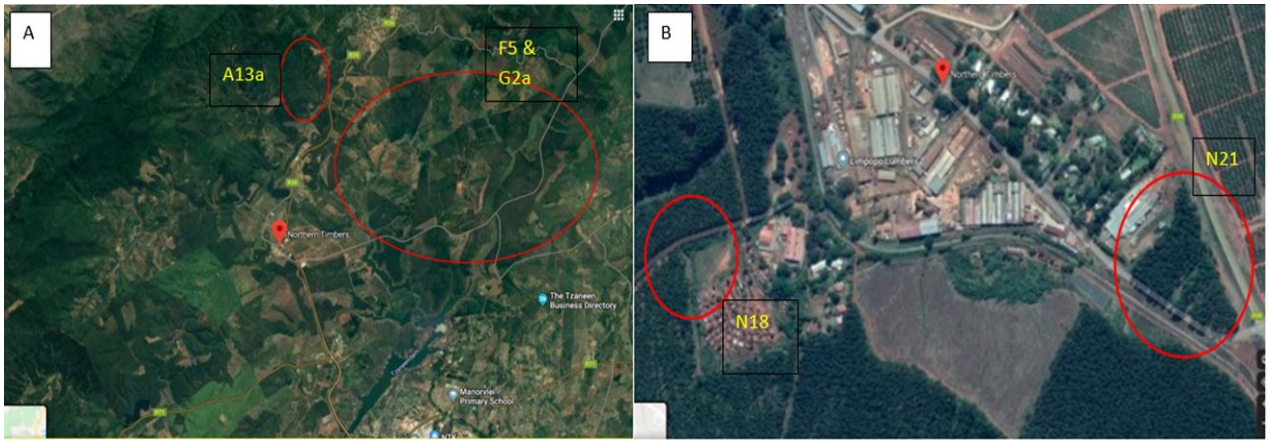

Figure 3- 1: Pictures showing plantation areas of Northern Timbers (Merensky) compartments (A) A13a, F5 and G2a and (B) N18 and N21.

Figure 3- 2: Picture showing (A) marking of the billets including north side and (B) marking of the north side on tree before felling.

Table 3- 1: The table with compartments characteristics and the data about the sampled material.

	F5	**N18**	**N21**	**N21**	**A13a**	**G2a**
Group	Young Improved (YI)	Young Unimproved (YU)	Matured Improved (MI)	Matured Unimproved (MU)	Splitting Trial (EX)	Old (OL)
Age Group (years)	8	7	13	13	17	24
Species	*E. grandis*	*E. grandis X E. urophylla*	*E. grandis*	*E. grandis X E. urophylla*	*E. grandis*	*E. grandis*
Site Index	51.6	54.8	43	43	53.9	54.8
MAI (m^3/ha/year)	28.57721	23.45318	27.97878	27.97878	N/A	22.81851
UMAI (m^3/ha/year)	24.19255	19.64236	24.10999	24.10999	N/A	19.66387
Est	Seedling	Clone	Seedling	Seedling	Seedling	Seedling
Spacing (m)	6.05	6.33	6.36	6.36	3.5	5.18
Comment	EP	GUY	EP	N/A	High/Low split part burnt	GUY
No. of trees	10	10	10	10	20	10
Map Coordinates	(23°41'49.8''S 30°05'27.4''E)	(23°46'10.2''S 30°05'54.7''E)	(23°45'54.2''S 30°06'27''E)	(23°45'54.2''S 30°06'27''E)	(23°43'50.2''S 30°07'01''E)	(23°42'20.6''S 30°06'33.8''E)
Seedstock	E/P	GXU 111	E/P	087 + 092 + 111 +10	SGR 483 + SGR 467	194033/0482

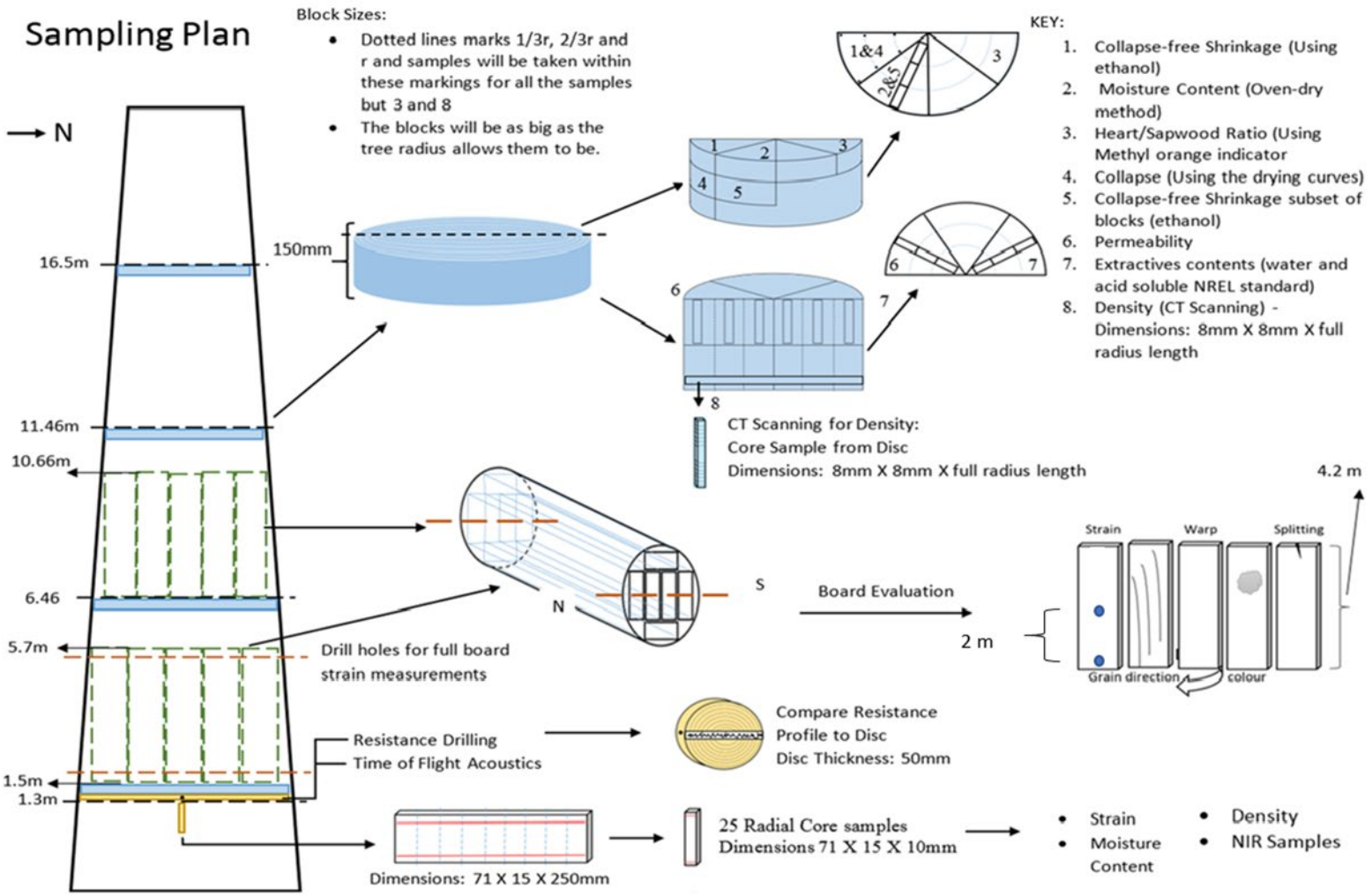

Figure 3- 3: The sampling plan for the study.

3.2 Methods

3.2.1 Shrinkage and collapse

For collapse and shrinkage, a wedge of 2cm thickness extending from pith to bark was removed from all four billets (see *figure 3-4*). The wedge was used to determine radial and tangential shrinkage and collapse from saturation to oven dry state. On each wedge, a marker was used to mark 1/3 of the radius, 2/3 of radius and at the end of the radius on both sides of the wedge. The lines connecting the dots/points at 1/3r, 2/3r and the end of the radius were also drawn as seen in *figure 3-4* below, which represented shrinkage in tangential direction (Wessels et al. 2016). The samples were then dried in a conditioned room (20° C and 60% relative humidity) until they reached equilibrium moisture content. The samples were repeatedly weighed and scanned throughout the drying cycle for about 3 months to measure drying rate (mass loss) and shrinkage. The samples were suspended by small sticks during drying to allow air flow on all sides as can be seen in *figure 3-5.* The scans of the samples were measured afterwards using image J software (Emaminasab et al. 2015). Using calculated dimensional changes from measurements of the scans and corresponding MC percentages the following method was used to compute collapse and collapse free shrinkage.

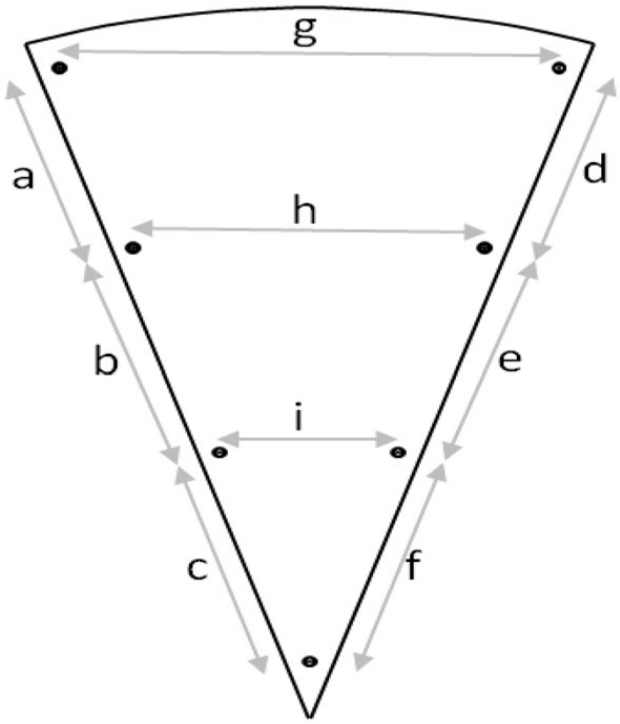

Figure 3- 4: Wedge with marks of measurements for shrinkage and collapse in radial and tangential directions.

Work by Wu et al. (2005 and 2006) has reported that normal shrinkage only occurs below FSP, and dimensional/volumetric changes observed above FSP are due to collapse only. FSP for most of the woods have been assumed around 28%. Furthermore Wu et al. (2005) reported that the shrinkage curves of the Eucalyptus species they have been working with that included *Eucalyptus grandis* were almost straight lines below about 28 % MC. Hence the equation to describe the curve below FSP can be (from Wu et al. 2005; 2006):

- $Y_1 = -\alpha.x + \beta_1$ ……*Equation 1*

Where Y_1 is the total shrinkage including residual collapse (%), x is the MC (%), α is the slope of the line described as the unit shrinkage and β_1 is the intersection with y-axis and expresses the largest shrinkage at 0% MC. To obtain collapse-free shrinkage (normal shrinkage), a straight line that coincides with FSP and parallel to *Equation 1* (Y_1) can be obtained as follows (from Wu et al. 2005; 2006):

- $Y_2 = -\alpha x + \beta_2$ ……*Equation 2*

Where Y_2 is the normal shrinkage (collapse-free shrinkage) at any MC below FSP, β_2 is the intersection with y-axis and the largest shrinkage at 0% MC, and α and x are still the same as in *equation 1*. Letting x be *28%* as FSP, then $Y_2 = 0$ since the normal shrinkage only takes place below FSP, therefore β_2 is solvable. Then the residual collapse will be calculated as the difference between β_1 and β_2 (Wu et al. 2005; 2006). *Appendix A figure 2* shows how the above calculations were done and graphs with the lines from the equations.

Figure 3- 5: Pictures of collapse and shrinkage samples during drying.

3.2.2 Collapse free shrinkage

From each disk at the four heights, a wedge was removed, extending from pith to bark similar to the ones for collapse (*see figure 3-4 and 3-5*). The wedge was used to determine radial and tangential shrinkage from saturation to equilibrium moisture content. On each wedge, points were marked at 1/3 of the radius, 2/3 of radius and at the end of the radius on both sides of the wedge. The three measurements between points represented shrinkage in tangential and radial direction (Wessels et al. 2016). To avoid collapse being part of the shrinkage measured (only measure collapse-free shrinkage) water was replaced by ethanol in freshly cut wood; as literature by Bariska (1992) reported that the incidence of collapse was remarkably reduced or completely eliminated by replacing water in freshly cut wood by organic liquids having lower tension than that of water. The samples were scanned, and Image J software was used to measure them. A sub-set of samples were also treated with ethanol, then blocks of 2*2*2 cm were cut between 2/3r and r. The blocks were used to determine shrinkage using the traditional method whereby the measurements were taken using a digital calliper in radial and tangential directions. The sub-set of blocks were compared to the corresponding wedges to see if the two methods give similar results.

3.2.3 Density

From each of the four billets a strip of 8 mm thickness extending from bark to bark was removed. The samples were dried to equilibrium moisture content (EMC) around 12% in a conditioning room before they were scanned with a CT scanner. To determine the density of an unknown material with the CT scan a homogenous sample must be scanned together with a calibration set (Freyburger et al. 2009; du Plessis et al. 2013). The calibration set is of a similar material with a known density. For this study four blocks of *Eucalyptus* and one of Pine with known densities were used for the calibration (*see figure 3-6 A*). The calibration samples must be of a range from low to high density. The grey values obtained from the scans were used to calculate the actual density. The scanning was done in a 2 mm interval from one end to the other. The profiles extended from bark to bark but, for the purpose of this study the profile extending from pith to bark on the north side of sample were taken then it was further averaged over 1/3r, 2/3r an r to compare with the rest of the properties.

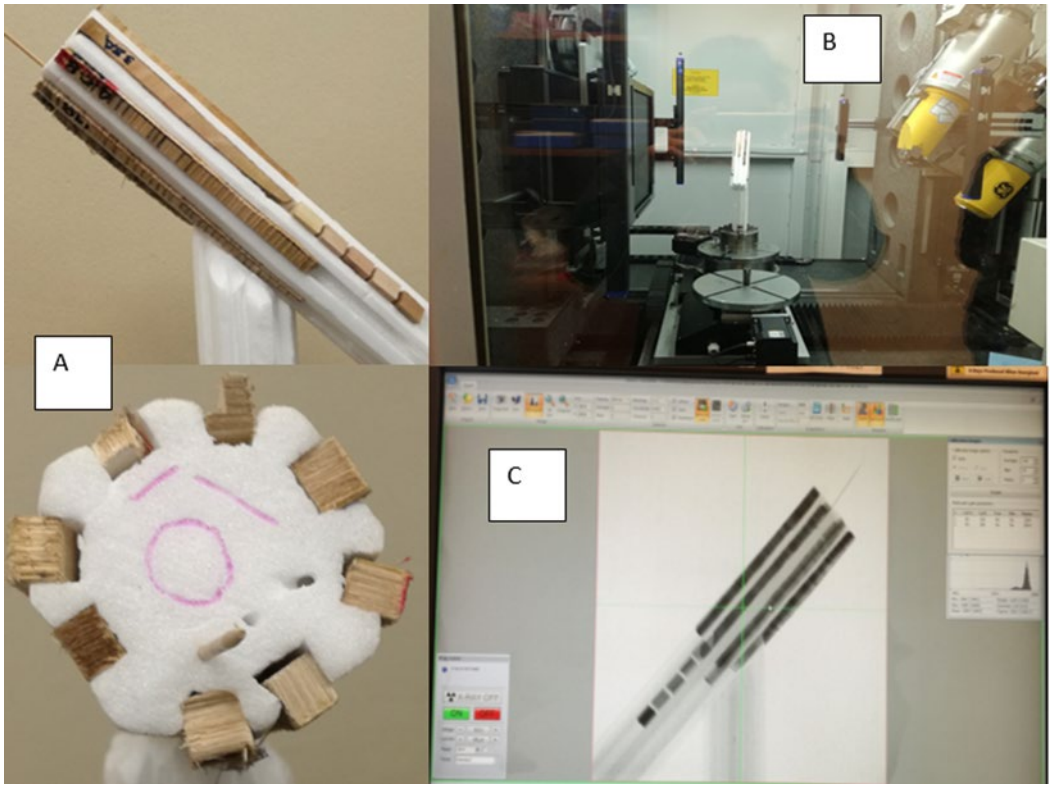

Figure 3- 6: Picture showing (A) density samples with the calibration samples on the handler, (B) samples inside the CT scanner and (C) the actual scanning on the computer screen and graphs resulting.

3.2.4 Heartwood/Sapwood ratio

Heartwood/Sapwood ratio is the amount of sapwood-compared to heartwood of the wood sample. In this study it was determined on a wedge extending from pith to bark according to Githiomi and Dougal (2012) using methyl orange indicator at 0.1% concertation, diluted with water (using a ratio

of 1g to 25 mL) to indicate the boundary between heartwood and sapwood. The solution was brushed on the surface from sapwood to heartwood to avoid the heartwood debris to contaminate the sapwood part and left to dry; thereafter, using a pen, the points at the heartwood sapwood boundary were marked. *Figure 3-7* shows the sample of the heartwood sapwood ratio test. The ratio was calculated by dividing the heartwood by the sapwood hence, higher ratios means high amount of heartwood and vice versa.

Figure 3- 7: The actual sample for heartwood/sapwood determination.

3.2.5 Moisture Content

From each billet a strip of 2*2 cm extending from pith to bark was removed and a 2*2*2 cm blocks were cut out (the number of blocks depended on the radius of each sample). The samples were weighed for wet mass (M_w) then oven dried at 103°C ± 2°C for 24 hours and then weighed again for the dry mass (M_d), oven dry MC% was calculated on the dry mass basis as per Tsoumis (1991).

3.2.6 Extractive contents

Water-soluble extractives were extracted using the TAPPI standard. Samples blocks from the heartwood, transition wood and sapwood (i.e. at 1/3, 2/3 and end of the radius) were milled and extracted separately for the determination of the variation of extractives from pith to bark as seen in *figure 3-8, (A)* the sketch as to where the samples were taken, *(B)* the milled sample and *(C)* the actual extraction. Extractives was done on a sub-set of 35 samples, and only samples at the breast were extracted. Every sample was extracted three times (3 replicates) to ensure that the value obtained is indeed correct.

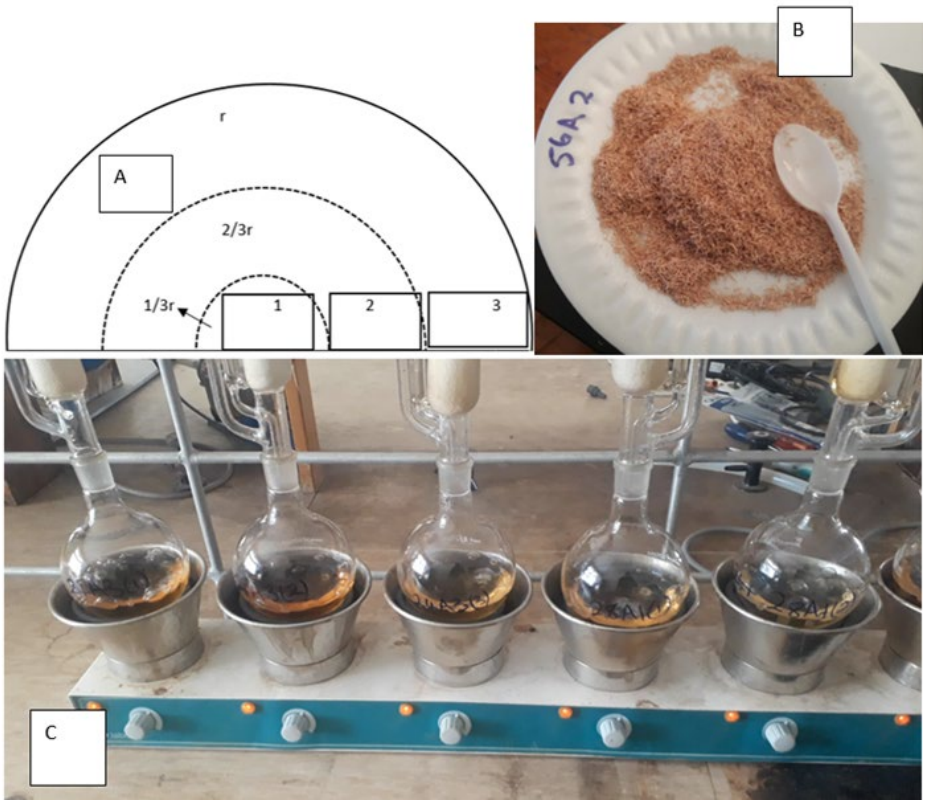

Figure 3- 8: (A) The sketch showing the extractives samples position, (B) samples after milling and (C) the actual extraction process.

3.2.7 Permeability

Three 2*2*2 cm blocks were cut from each of the four billets (*see figure 3-9 B*) one within 1/3 of radius, one within 2/3 of radius and one after 2/3r and end of radius a total of 840 samples was used for permeability. The 3 blocks represented the 3 radial positions similar to that of shrinkage on the wedges. The blocks were allowed to dry to EMC (about 12%) then the longitudinal ends were coated (sealed) with polyurethane resin to ensure that water only move radially and tangentially (Emaminasab et al. 2015). The blocks were then submerged in water and cycles of vacuum and pressure (100kPa and 600 kPa respectively) were applied until the samples were saturated with water. The samples were then dried in the conditioning room at 20°C and 60%

relative humidity keeping them upright exposing all uncoated sides to air as can be seen *in figure 3-9 (A)*. The samples were all weighed 5 times during the drying cycle until EMC was reached with a constant time between each weighing event. The difference in the mass between weighing samples were used to calculate a drying gradient (mass loss/time) between each weighing event and subsequently a drying curve for each sample. The gradient for each sample was calculated and they were based on the percentage of the mass lost to standardize them and avoid difference in mass to influence the slope i.e. the percentage was calculated based on the maximum mass of the sample fully saturated. The drying curves method was used to determine the permeability of the samples. Based on the slope of the drying curve it was deduced which sample lost water faster within a fixed period i.e. if the sample lost water faster the slope of the drying curve would be steep while for the samples that lost water slow the slope will be gentle.

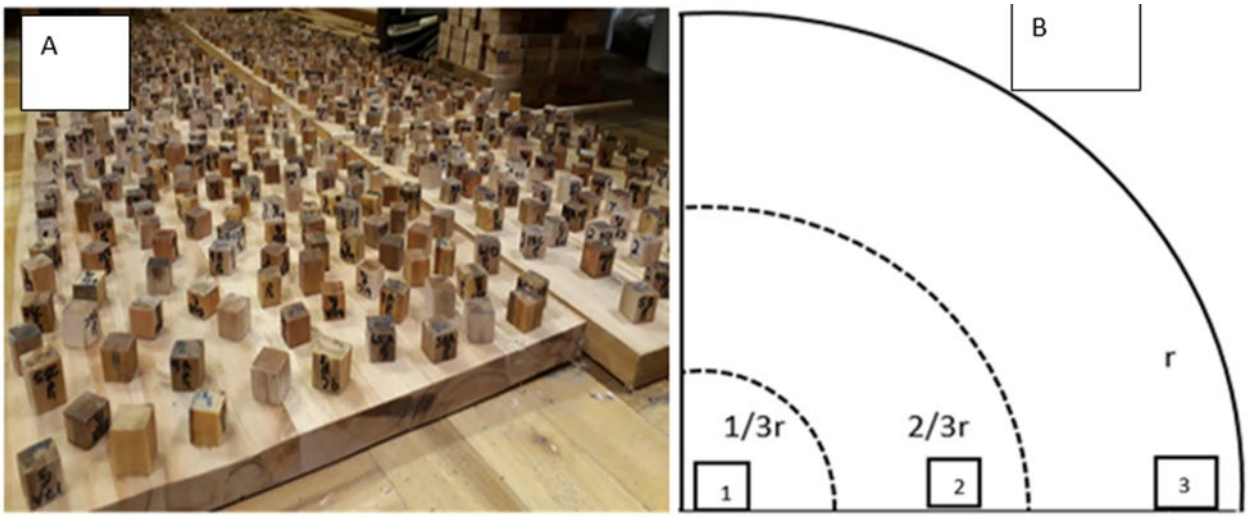

Figure 3- 9: The picture showing (A) permeability samples and how they were stored and (B) a sketch showing where they were taken in the tree disk.

3.2.8 Shrinkage and collapse – boards

Collapse was visually assessed on the surface of the boards and the percentage of the surface with visual traces of collapse was recorded (see *figure 3-10 A)* below. The worst surface was assessed between the bottom and top surfaces.

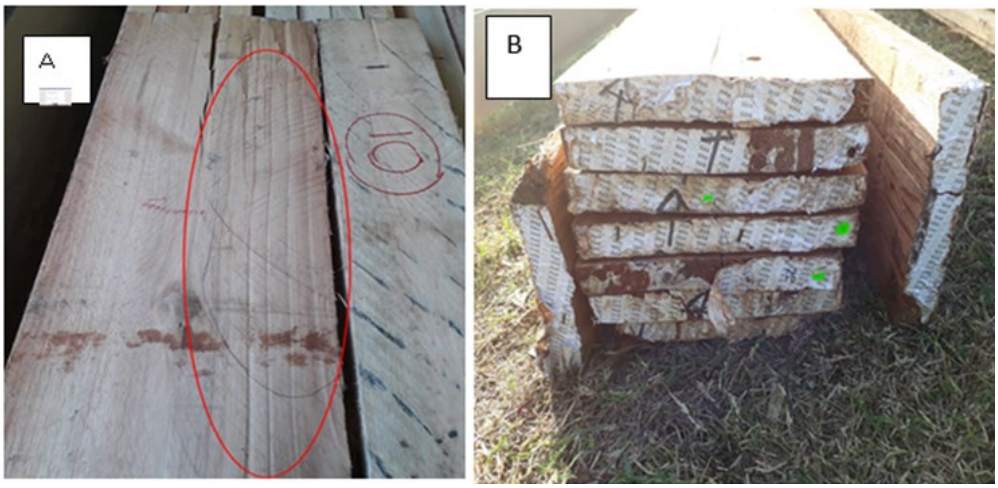

Figure 3- 10: Visual assessment of collapse on the boards (A) and the reconstruction of boards (B).

For shrinkage the boards were marked at 3 places from lower end of the log to the higher end of the log as can be seen on *figure 3-10 (A).* However, the marks were not equally spaced due to the defects such as splitting that were avoided. Using the digital calliper, the measurements of the thickness and width at the marked points were taken before and after drying and the difference between the measured dimensions was used to calculate the shrinkage as a percentage. In *figure 3-11* (B) the jig that was used as the working table for measuring the boards is shown. The jig was made from aluminium and was 4.2 m long and the two pins were just less than 4.2 meters apart to allow for measurements. Cup was measured using a T-square with one of its flat surfaces put across the surface of the board, then the space between the board and the T-square was measured using the ruler. For bow the ends of the board were put against the pins of the jig (with the width side against the pins) and the deflection from the straight piece of aluminium was recorded as bow. Twist was measured at the ends of each board as seen in *figure 3-11 (C)* by taking the distance between the jig and the lifted side of the board. The boards were later assembled back into their respective logs using the stickers at their ends and aligning the defects on their surfaces to create the profiles across the logs as can be seen in *figure 3-10 (B)* above.

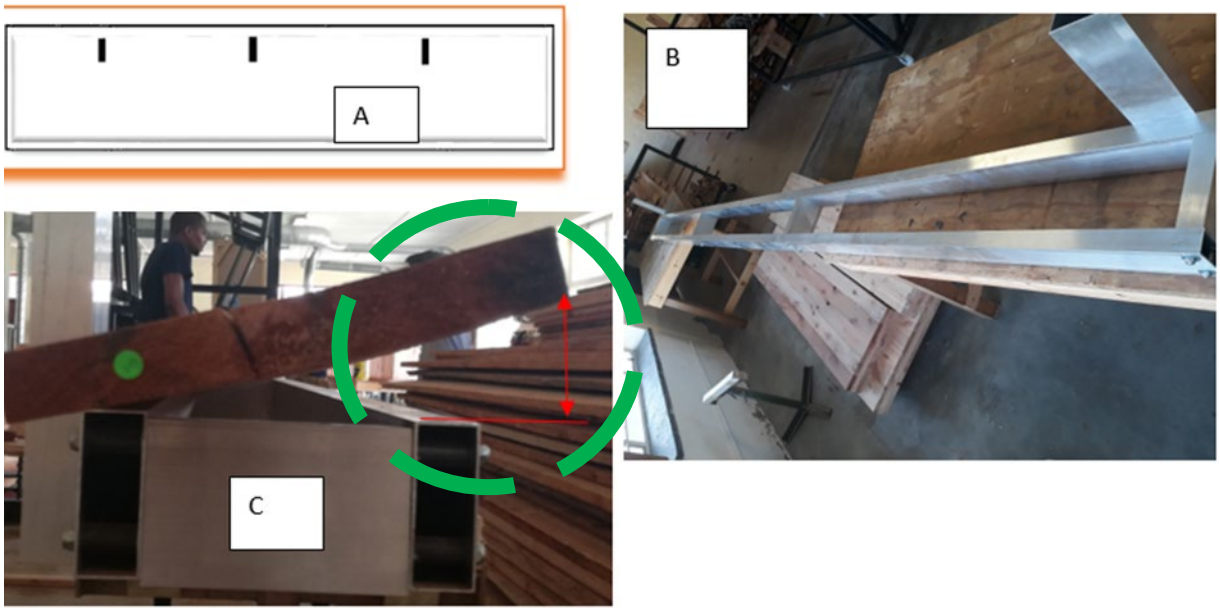

Figure 3- 11: The picture showing how the measurements of shrinkage, bow and twist were performed.

3.4 Statistical Analysis

RStudio (R Statistical software) was used for the analysis of the results from the study. Three-way factorial analysis of variance (ANOVA) was used. The input factors for properties measured on the samples wedges were Groups (YI, YU, MI, MU, EX, OL) ; Heights (A, B, C, D) and Radial Positions (1, 2, 3). The input factors for the boards were Groups (YI, YU, MI, MU, EX, OL) ; Logs (A and B) and Radial Positions (0, 1, 2, 3). The factor groups was used to compare the elite population (improved trees) and unimproved trees, also to show the effect of age (young, mature, and old). Heights and Logs gave the effect of heights - A being the breast height and D the highest sample obtained, and log A being the first log in the tree then B the second log. Radial Positions gave the radial effect from pith to bark. The 3-way ANOVA was used to evaluate the effect of the variables on the response variables (Collapse, Shrinkage, Density, MC, Permeability, Extractives Contents, Heart/Sap wood ratio, Twist, Bow and Cup) and their interactions with each other. The highest order of significances were displayed in graphs to represent the findings of the study.

The linear models (lme and lmer) from packages nlme and lme4 respectively were used for samples and boards respectively as the boards data was highly unbalanced. The residuals of the models were checked for normality and all the data in the study was normally distributed. Furthermore ; fixed effects were set in the models to avoid pseudoreplication of the factor tree. A Pearson correlation matrix was used to determine the correlations between variables. Linear regression and multiple linear regression were performed to evaluate the relationships between variables and develop prediction models for collapse and shrinkage.

The ANOVA's was performed using the alpha (α) value of 0.05 hence, the error bars in the graphs displayed in the next chapter represents the 95% confidence interval. The p-values are displayed in the tables for each of the variables that were tested and all the significant p-values are highlited in green. The null hypotheses that was tested was that the variables or the interaction are all the same (not significant) and the aternative hypotheses was that atleast one of the variables is different.

The two-sample t-test was used to test whether the means between two methods (wedges and blocks) were different. The null hypothesis was that the difference between the two means is zero (they are equal). The boxplots were also plotted to visually show how the means differs. The data for radial shrinkage passed the normality test and variance test while, the tangential data only blocks passed the normality test. Wedges were not normally distributed as a result the Wilcoxon Sum Rank test was used.

Chapter 4: Results and Discussions

In this section, results of properties that might have an influence on shrinkage and collapse behaviour are presented first. After that the actual shrinkage and collapse results were presented and discussed together with possible relationships between properties. The alphabetic letters on the graphs show the significant differences between points i.e. different letters indicate means that were significantly different while similar letters mean no significant difference was observed. The bars display 95% confidence intervals.

4.1 Density

The data for density was normally distributed and the lme () function in R was used to analyse the data. *Table 4-1* shows that all variables were highly significant and the interaction between radial position and groups as well. The graphs of interaction between radial position and group; and the effect of height were displayed below in *Figures 4-1 and 4-2*.

Table 4- 1*:* The ANOVA table for density.

Density

	Random effects: Formula: ~1 | Tree			
Std Dev:	Intercept 57.58595	Residual 65.99306		
Effect	NumDF	denDF	F-value	p-value
Intercept	1	437	4510.795	<.0001
Radial Position	2	437	28.421	<.0001
Height	3	437	15.221	<.0001
Group	5	58	1.926	0.0827
RadialPosition:Height	6	437	1.650	0.1319
RadialPosition:Group	10	437	3.597	<0.0001
Height:Group	15	437	1.610	0.0433
RadialPosition:Height:Group	30	437	0.592	0.9591

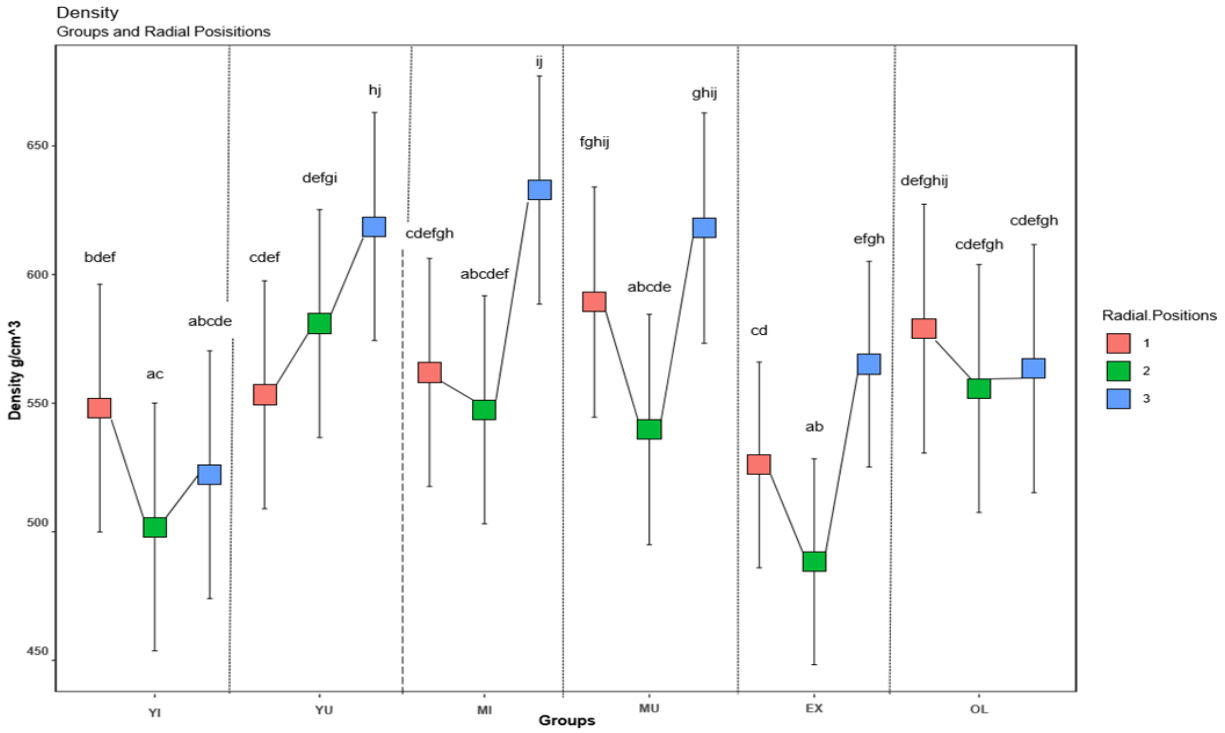

Figure 4- 1: The interaction between group and radial position for density the letters in graph shows the significant difference between points.

The trends observed in *figure 4-1* is almost similar for all the groups except the young unimproved group. (Bhat et al. 1990; Wilkins et al. 1991; Githiomi et al. 2010) found similar trends and reported that the radial variation of density curve of *E. grandis* initially declined from pith, before it gradually increases towards the bark forming a v-shaped curve. However, the trend observed for the young unimproved group followed results reported by a number of authors for other species including Gierlinger et al. (2004) for *European larch* trees. The difference between improved trees and unimproved trees was quite visible for young trees, as it is evident from *figure 4-1* in the means of positions 2 and 3 for the two groups. The trees from the splitting trial (EX) which were aged between mature groups and the old group showed the same trend but with lower means. The old group (OL) showed a similar trend, however, there were no significant difference between the 3 radial positions which means it had greater uniformity.

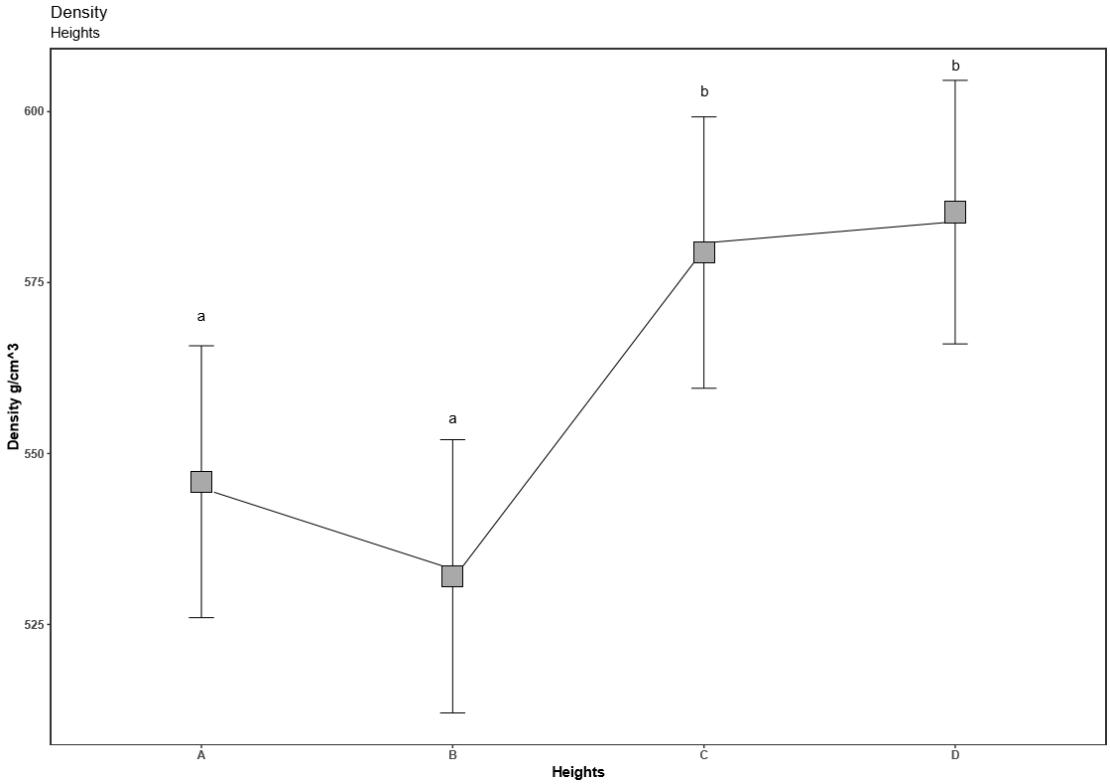

Figure 4- 2**:** The effect of height on density.

Figure 4-2 showed that density at breast height and 6.4 m was lower than the two top positions. A similar trend for *Eucalyptus grandis* has been reported by (Bhat et al. 1990; Wilkins et al. 1991; Githiomi et al. 2010) who reported a decline from stump height up to 25% of the tree height and then a gradual increase to the top of the tree. However, there was no significant diffence between the first two heights (A and B) as the top two heights (C and D) were similar as well. Density values ranged from 450-650 kg/m^3 and they are comparable to values reported by Bhat et al. (1991) of 495 kg/m^3; Sharma et al. (2015) of 442 kg/m^3 and Pagel (2019) of 500-600 kg/m^3.

4.2 Heartwood-sapwood ratio

The data was normally distributed and the lme () function in R was deemed appropriate to analyse the data. The results showed no significant interaction between height and group; however, the main effects of height and group were both highly significant (*see Figures 4-3 and 4-4*).

Table 4- 2*:* The ANOVA table for heartwood/sapwood ratio.

Heartwood Sapwood Ratio

	Random effects: Formula: ~1 | Tree			
	Intercept	Residual		
Std Dev:	0.6319198	0.6712135		
Effect	NumDF	denDF	F-value	p-value
Intercept	1	177	1722.4967	<.0001
Height	3	177	74.0165	<.0001
Group	5	64	37.0244	<.0001
Height:Group	15	177	0.4472	0.9624

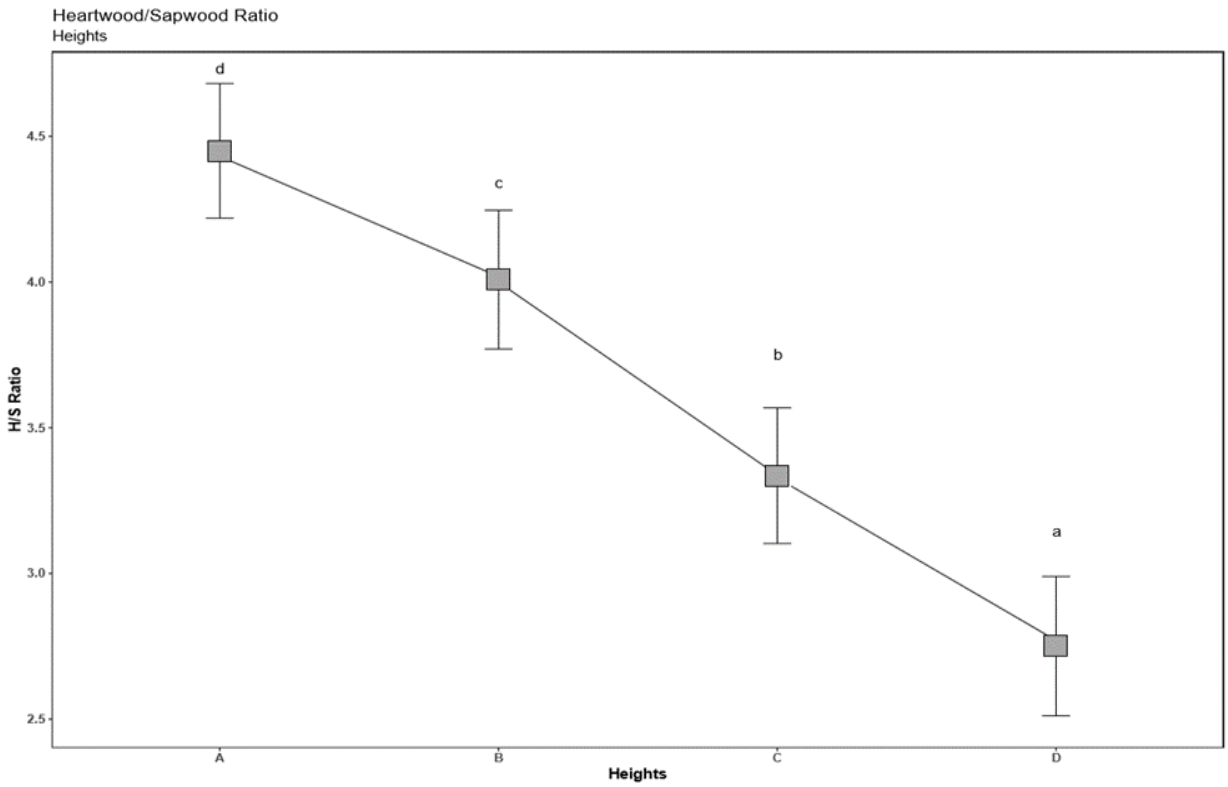

Figure 4- 3: The effect of height on heartwood/sapwood ratio.

Figure 4-3 shows a consistent decline in the heartwood sapwood ratio from breast height (A) to 16.52 m (D). This was expected as the breast height is the part of the tree with more heartwood and the top part of the tree mostly comprises of the newly formed wood which is sapwood. These findings are in line with findings of Morais et al. (2007) and Kumar et al. (2014) on *Eucalyptus* species. Further, Kumar et al. (2014) found that the taper of heartwood was more than that of the tree. All 4 heights were significantly different from one another. This also gives an expectation that properties that depend on heartwood and sapwood behaved according to this observed trend i.e. density, collapse and shrinkage might be influenced by this ratio and might subsequently differ from height A to height D.

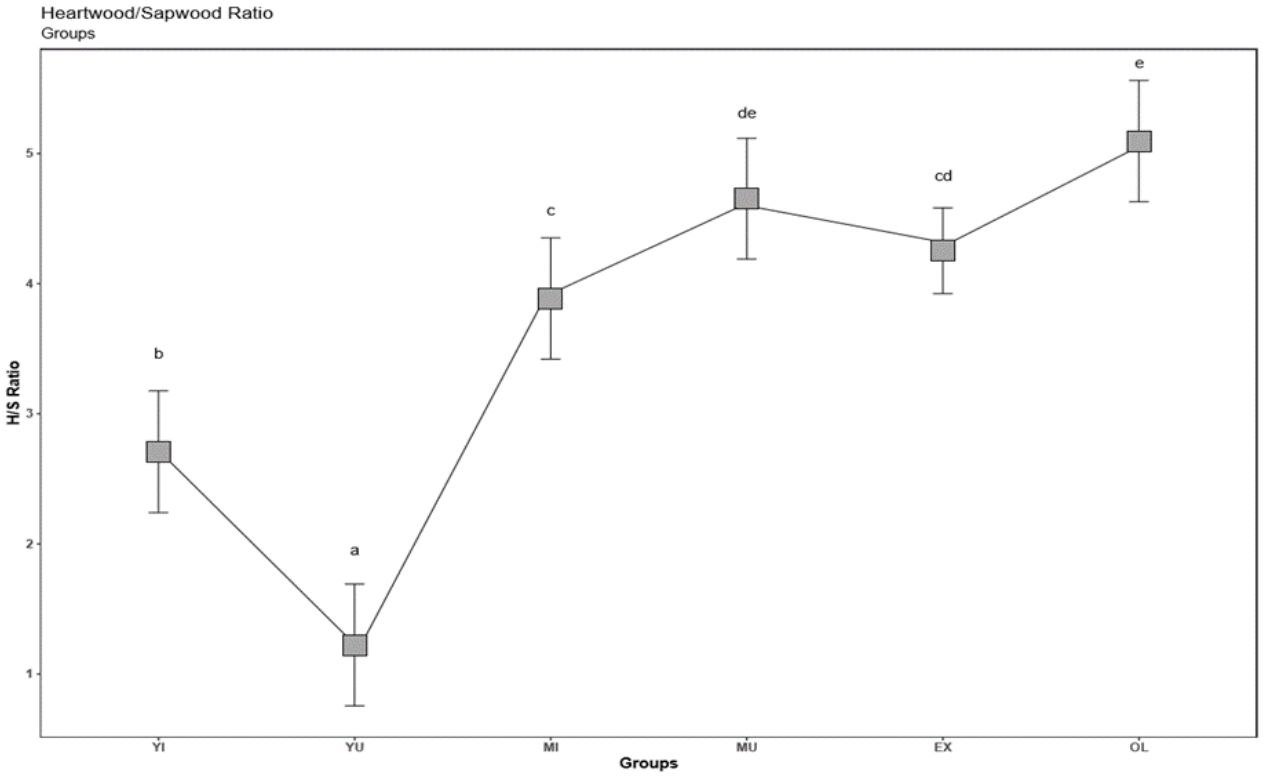

Figure 4- 4: The effects of groups on heartwood/sapwood ratio. For an explanation of groups, see Table 3-1.

Figure 4-4 shows the effects of different groups on the heartwood/sapwood ratio. Groups varied according to age, species, and genetic improvement. It is clear from the graph that age had an effect as the young groups (YI and YU) had a high amount of sapwood compared to the mature (MI and MU) and old groups (EX and OL). Further, there was a significant difference between young improved trees and unimproved trees with unimproved trees having more sapwood than improved trees. The variation of the heartwood/sapwood is influenced by the number of factors including species, age, growth rate, tree foliage, genetics, and environmental factors such as soil, climate, site quality, tree vitality and forest management (Miranda et al 2006; Morais et al. 2007; Sabrina et al. 2018). For the young age group the unimproved trees had more sapwood compared to improved trees - this might be due to the slow growth of the unimproved tree as the formation of heartwood also depends on the growth rate. However, this changed at the mature age group and may be due to the genetic material. According to Kumar et al. (2014) in *Eucalyptus* heartwood formation starts as early as 3 to 5 years. Miranda et al. (2006) and Morais et al. (2007) stated that heartwood is formed when sapwood transforms into heartwood, with extractives accumulating and that part of the tree and cells becoming inactive (cells die). The mature improved trees had similar H/S ratio as the old trees - Kumar et al. (2014) links heartwood development to tree size so much that even aged trees that grows more in diameter than height have more heartwood. Morais et al. (2012) stated that for the same age, sites with fast growth rate had higher proportions of heartwood.

4.3 Moisture content

The moisture content data was distributed normally and the lme () function was used to analyse the data. *Table 4-3* shows that the interaction effects of height, group and radial position were highly significant.

Table 4- 3*:* The ANOVA table for moisture content.

Moisture Content

Random effects:
Formula: ~1 | Tree

	Intercept	Residual
Std Dev:	12.21082	12.3654

Effect	NumDF	denDF	F-value	p-value
Intercept	1	669	4350.090	<.0001
Radial Position	2	669	3.368	0.0350
Height	3	669	345.663	<.0001
Group	5	64	20.128	<.0001
RadialPosition:Height	6	669	8.542	<.0001
RadialPosition:Group	10	669	10.351	<.0001
Height:Group	15	669	9.375	<.0001
RadialPosition:Height:Group	30	669	1.302	0.1316

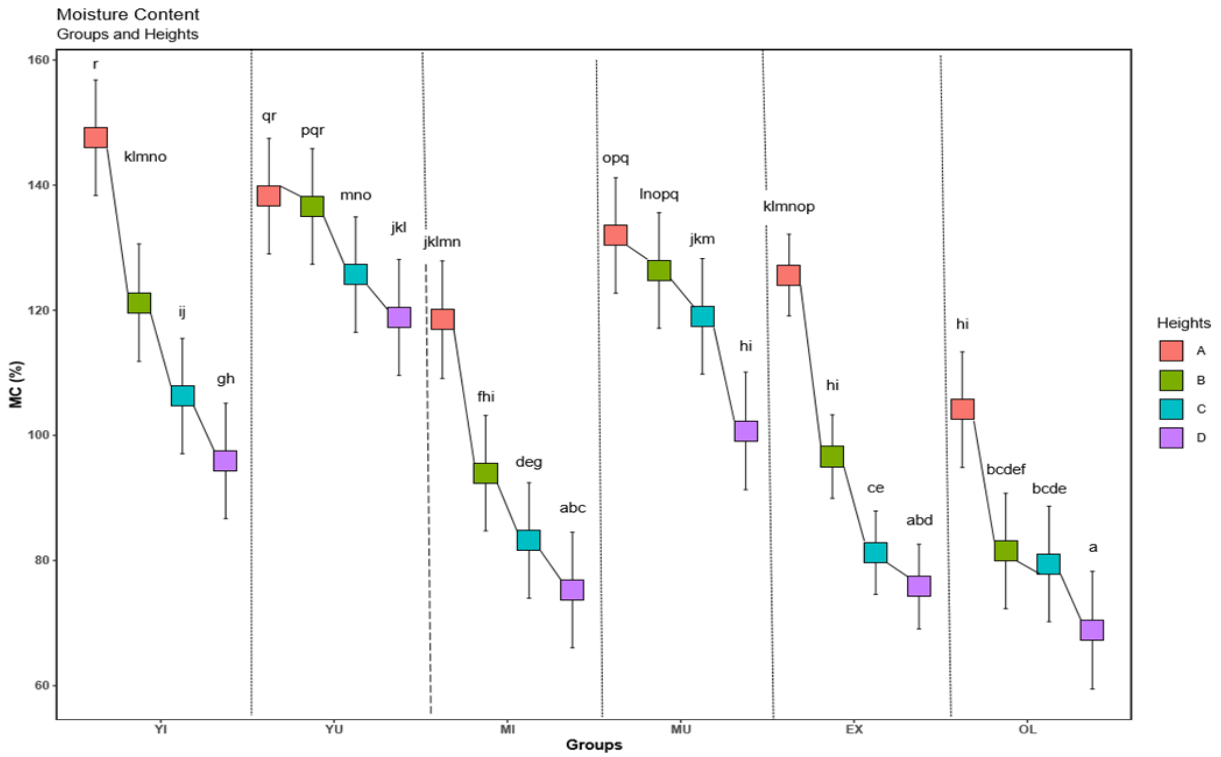

Figure 4- 5: The interaction between heights and groups for MC.

The trend observed in *figure 4-5* is consistent through all the groups and it is clear that moisture content decreased with height this might be due to the fact that at the top leaves continuously uses water for photosynthesis. Similar results were found by Zanuncio et al. (2015) for *Corymbia citriodora* and *E. urophylla*. For *E. grandis* a similar trend was reported by others (Oliveira et al. 2005; Engelund et al. 2013; Zanuncio et al. 2015). They further stated that the amount and distribution of MC in the longitudinal direction may vary based on the genetic material. From *figure 4-5* the effect of age is observed as both the young groups had the highest MC at breast height and the oldest group had the lowest MC. The genetic effect (improved and unimproved trees) is seen improved groups (YI and MI) seems to have large changes in MC from height A to B while the unimproved groups (YU and MU) had a more gradual change in MC. It can be concluded that MC was a function of age as it appears to decrease with age from YI and YU to MI and MU also to OL. This may be explained by the fact that older trees had more heartwood than sapwood which is primarily responsible for water transportation see *figure 4-4*.

4.4 Extractives contents

The data was normally distributed and the lme () function in R was used to analyse the data. The results showed that group was not significant but the interaction between group and radial position was significant (*Table 4-2 and Figure 4-3*).

Table 4- 4*:* The ANOVA table for extractives contents.

Extractives Content

Effect	NumDF	denDF	F-value	p-value
Intercept	1	56	488.7048	<.0001
Radial Position	2	56	53.1328	<.0001
Group	5	28	1.5575	0.2045
RadialPosition:Group	15	56	5.3194	<.0001

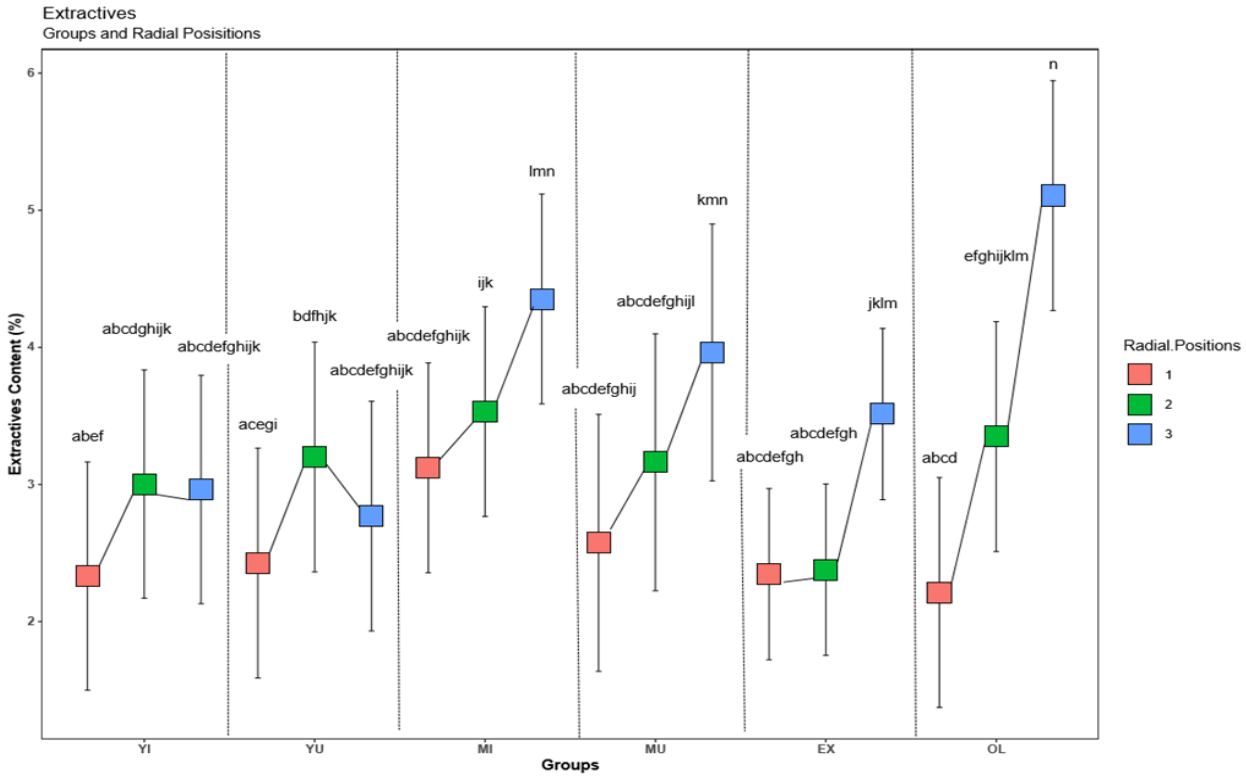

Figure 4- 6: The interaction between groups and radial positions for hot water extractives contents.

Figure 4-6 clearly shows a non-uniform trend between groups. However, the effect of age is quite notable with young groups having a different trend from that of mature and old groups. The study only investigated the hot water-soluble extractives content and did not include the ethanol or dichloromethane soluble extractives. The increase of extractives contents from pith to bark was unexpected as most literature suggested that more extractives contents are found in the pith due to presence of heartwood where they accumulate during its formation (Cherelli et al., 2016). However, Gierlinger et al. (2004) reported in contrast that extractives of European larch increased from pith to bark. Miranda et al. (2011) reported that *Tectona grandis* extractives contents comprised of 85% ethanol and dichloromethane soluble extractives and only 15% water soluble extractives for the heartwood, with sapwood having 68.47% ethanol and dichloromethane soluble extractives and 31.52% water soluble extractives. If *Eucalyptus grandis* and *Eucalyptus grandis X urophylla* behave similarly, it may explain the increase from pith to bark of the hot water extractives contents observed in this study. Furthermore Lloyd (1978) and Miranda et al. (2011) stated that a high amount of polar compounds is found in sapwood (close to the bark) which is associated with the metabolic activities observed in the transition zone of the tree. This may be related to heartwood formation with the enzymic hydrolysis of triglycerides during the process and an increase in the fatty acids during the process of parenchyma cell death which can explain the different trend observed in young trees as well, since the heartwood formation may not be as fast. Lloyd (1978) also states that metabolic activities are governed by seasonal variations as they are formed during growth seasons and are consumed during winter. The samples of this study were

obtained in the middle of the growing season which could explain an increased amount of these compounds as seen in the graph above. Therefore, the trend of the total extractive's contents can possibly be assumed to still decrease from pith to bark. In hindsight, measuring of only hot water extractives might not capture extractives content sufficiently and it is suggested that future studies rather measure total extractives content if possible. With the current data it is difficult to make firm conclusions on the influence of extractives on other properties if there is a possibility that hot water extractives capture a relatively small amount of total extractives content.

The young groups (YI and YU) did not have a significant radial difference between radial positions except for radial position 1 and 2 for YU. The radial difference was significance for mature and old groups with radial position 3 being the highest for all 3 groups.

4.5 Permeability

Table 4-5 shows the ANOVA for permeability. The data was normally distributed and the lme () function was used to analyse the data. The interactions between radial position, height and group were highly significant. Hence, the graphs showing the interactions are shown below:

Table 4- 5*:* The ANOVA table for permeability.

Permeability

	Random effects: Formula: ~1 | Tree	
Std Dev:	Intercept 2.002633	Residual 4.946646

Effect	NumDF	denDF	F-value	p-value
Intercept	1	632	1736.6400	<.0001
Radial Position	2	632	11.8105	<.0001
Height	3	632	5.8021	0.0006
Group	5	64	4.8774	0.0008
RadialPosition:Height	6	632	3.1108	0.0052
RadialPosition:Group	10	632	2.5980	0.0043
Height:Group	15	632	1.3537	0.1647
RadialPosition:Height:Group	30	632	0.7834	0.7906

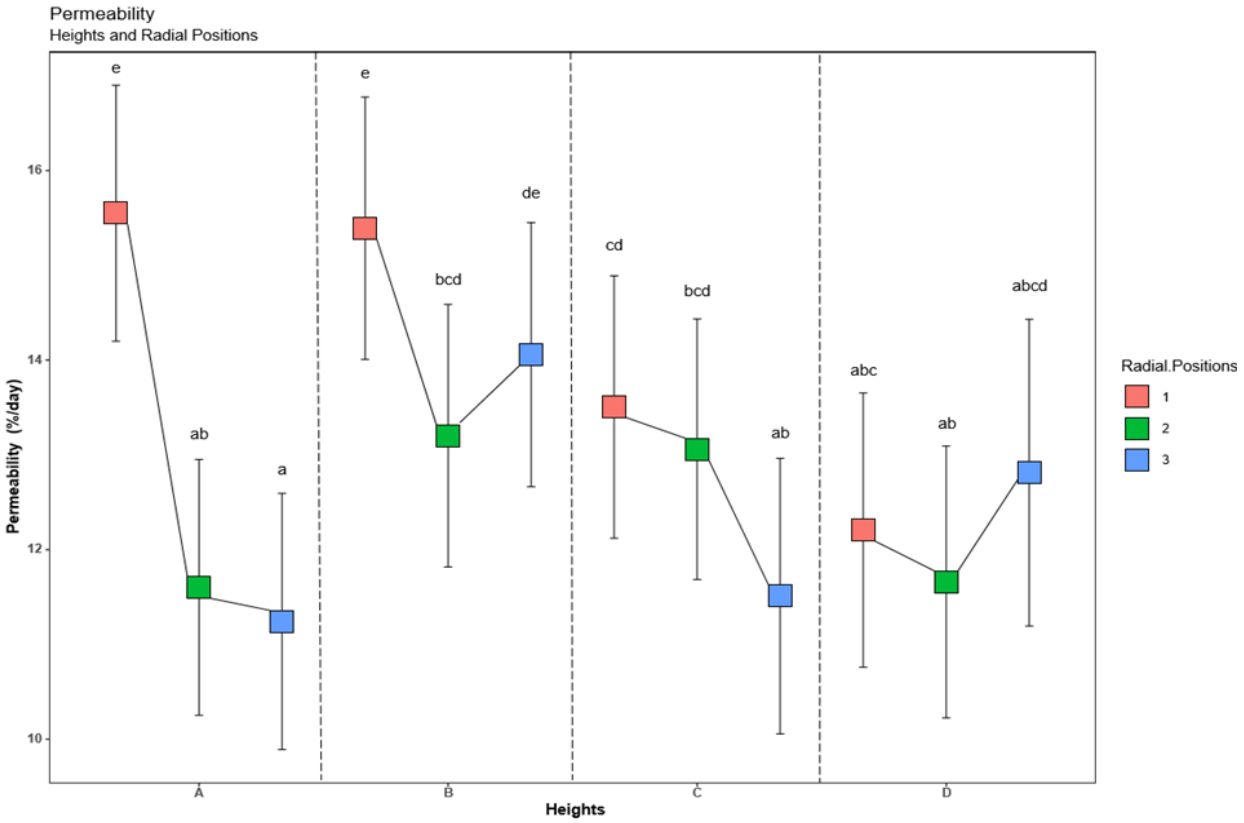

Figure 4- 7: The interaction between radial positions and heights for MC.

Figure 4-7 shows the interaction between radial positions and heights for permeability. The trend observed in this graph contrasts the commonly observed trends in literature including findings by Cherelli et al. (2018) where they reported heartwood being less permeable and having more compact tissue than sapwood. Literature suggest this specific trend especially for longitudinal permeability. According to Chafe (1978) wood is more permeable due to presence of vessels. However, in *Eucalyptus* tyloses may resist the flow through the vessels. Panigrahi et al. (2018) reported that longitudinal permeability is much higher than radial and tangential permeability and links permeability to density (higher density is associated with low permeability). However, the most distinct factor that has been suggested as hindering permeability in the heartwood is the presence of extractives which closes the pathways in vessels and fibres. The results shown in the graph do not show consistent radial variation. At breast height there was extreme radial variation, with less radial variation at other heights. Given the trend observed in extractives contents for these samples - higher values at the pith and lower values on the sapwood part - the permeability possibly mirrors that.

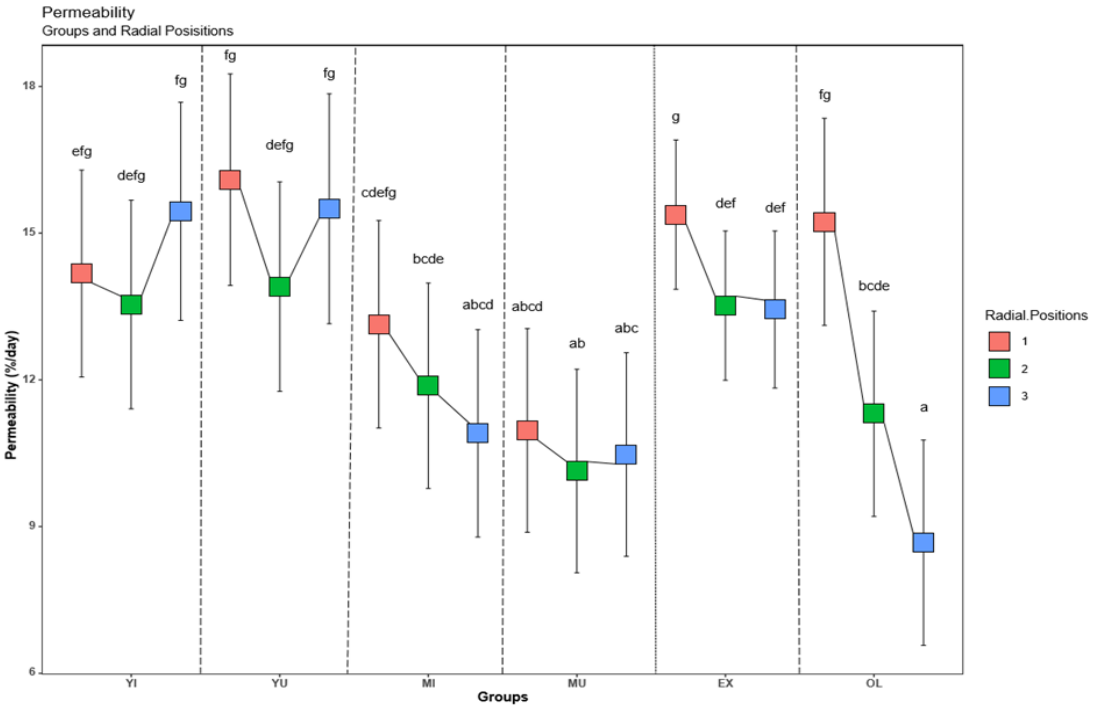

Figure 4- 8: The interaction between radial positions and groups for permeability.

Figure 4-8 shows the interaction between radial positions and groups for permeability. The younger groups (YI and YU) generally had higher permeability than the mature groups (MI and MU). The old group (OL) had extremely high radial variability. It is interesting to note that the radial positions / groups interaction graph of permeability (*Figure 4-8*) is nearly a mirror image of the hot water extractives graph (*Figure 4-3*). This seems to suggest that extractives have a large influence on permeability. However, the correlation between the two was not significant (*Table 4-16*) and will be discussed later.

4.6 Collapse

4.6.1 Disc samples (Radial)

The data for radial collapse was normally distributed and the function lme () was used to analyse the data. *Table 4-6* shows that all the effects were significant and the interactions between group, radial position and height were highly significant. There were no firm conclusions that could be drawn from the interaction of height and groups as a result only the graph showing the interaction between radial position and height is shown below:

Table 4- 6*:* The ANOVA table for radial collapse.

Radial Collapse

Random effects: Formula: ~1 | Tree				
	Intercept	Residual		
Std Dev:	0.3113047	0.710033		
Effect	numDF	denDF	F-value	p-value
Intercept	1	662	2815.1978	<.0001
Radial Position	2	662	195.5458	<.0001
Height	3	662	3.2044	0.0228
Group	5	64	16.8067	<.0001
RadialPosition:Height	6	662	1.9160	0.0759
RadialPosition:Group	10	662	14.9239	<.0001
Height:Group	15	662	2.4428	0.0018
RadialPosition:Height:Group	30	662	0.8445	0.7062

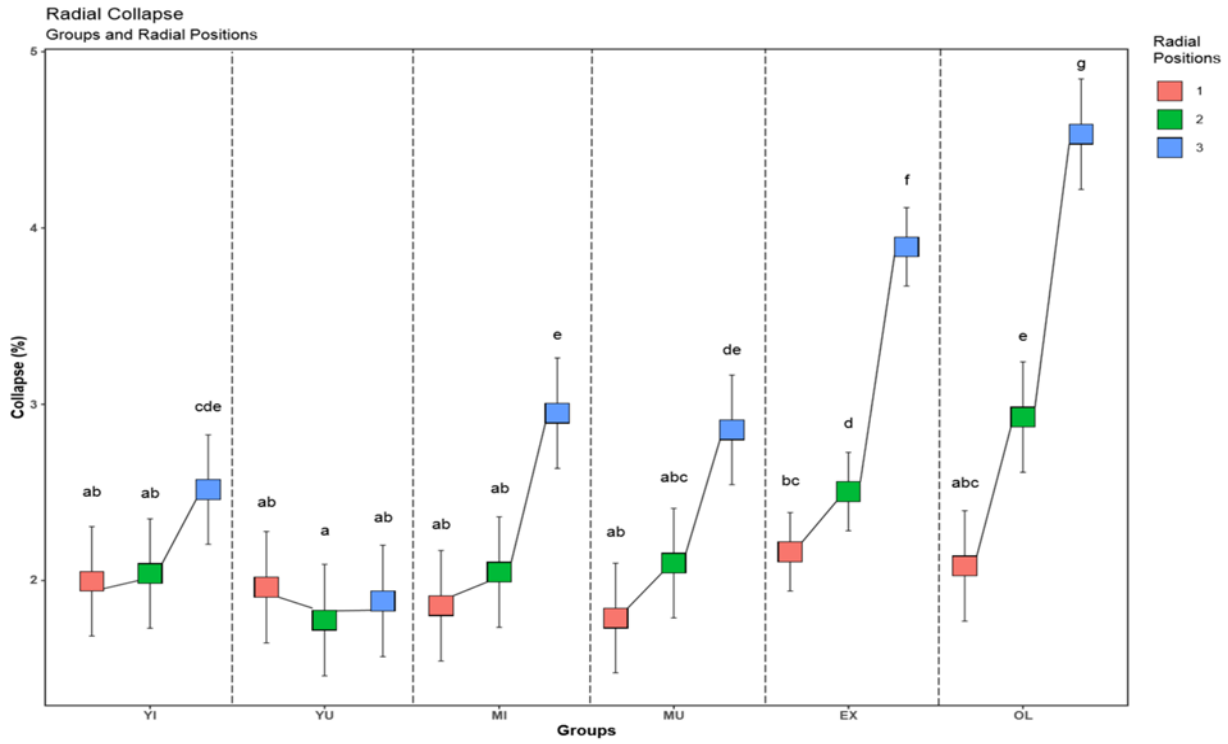

Figure 4- 9: The interaction between groups and radial positions for radial collapse.

Figure 4-9 shows the significant radial variation for all groups except YU, with radial position 3 always being the highest and significantly different for radial position 1 and 2. There is a trend of increasing radial variation in radial collapse.

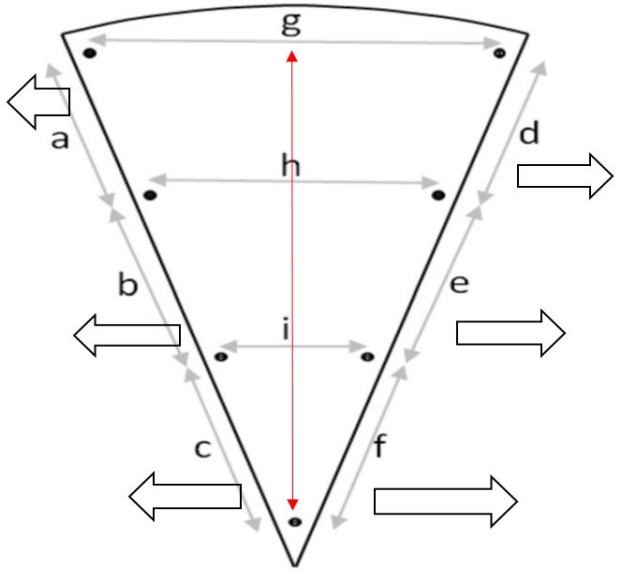

Figure 4- 10*:* Sketch of the collapse sample showing the possible water movements and sample size.

The trends observed in *figure 4-9* were not the expected trends suggested by the literature hence, the method used was subject to scrutiny. Kauman (1960) in Priadi (2001) reported that collapse

was found to be high on the width of rectangular samples compared to the cubic samples, also Greenhill (1936) in Yang et al. (2003) also stated that the measurement of collapse required a thin section usually of the order 1 mm as thin sections does not collapse. This indicates that size of the sample affects the measurement of collapse as can be seen in Figure 4-10 that the size of the sample at position 1 was considerably smaller than the other two positions. Further position 2 was smaller than position 3. Also, from Figure 4-10 it can be seen that the radial measurements were taken on the edge of the sample where there is an immediate opening for the water to leave wood.

4.6.2 Disc Samples (Tangential)

The data for tangential collapse was normally distributed and the lme () function was used to model and analyse the data. *Table 4-7* shows that the main effects of the variables and first order interactions were all highly significant.

Table 4- 7*:* The ANOVA table for tangential collapse.

Tangential Collapse

Random effects: Formula: ~1 | Tree				
	Intercept	Residual		
Std Dev:	0.4892288	1.181478		
Effect	NumDF	denDF	F-value	p-value
Intercept	1	662	4126.394	<.0001
Radial Position	2	662	64.485	<.0001
Height	3	662	95.313	<.0001
Group	5	64	8.150	<.0001
RadialPosition:Height	6	662	10.289	<.0001
RadialPosition:Group	10	662	8.569	<.0001
Height:Group	15	662	3.619	<.0001
RadialPosition:Height:Group	30	662	0.817	0.7452

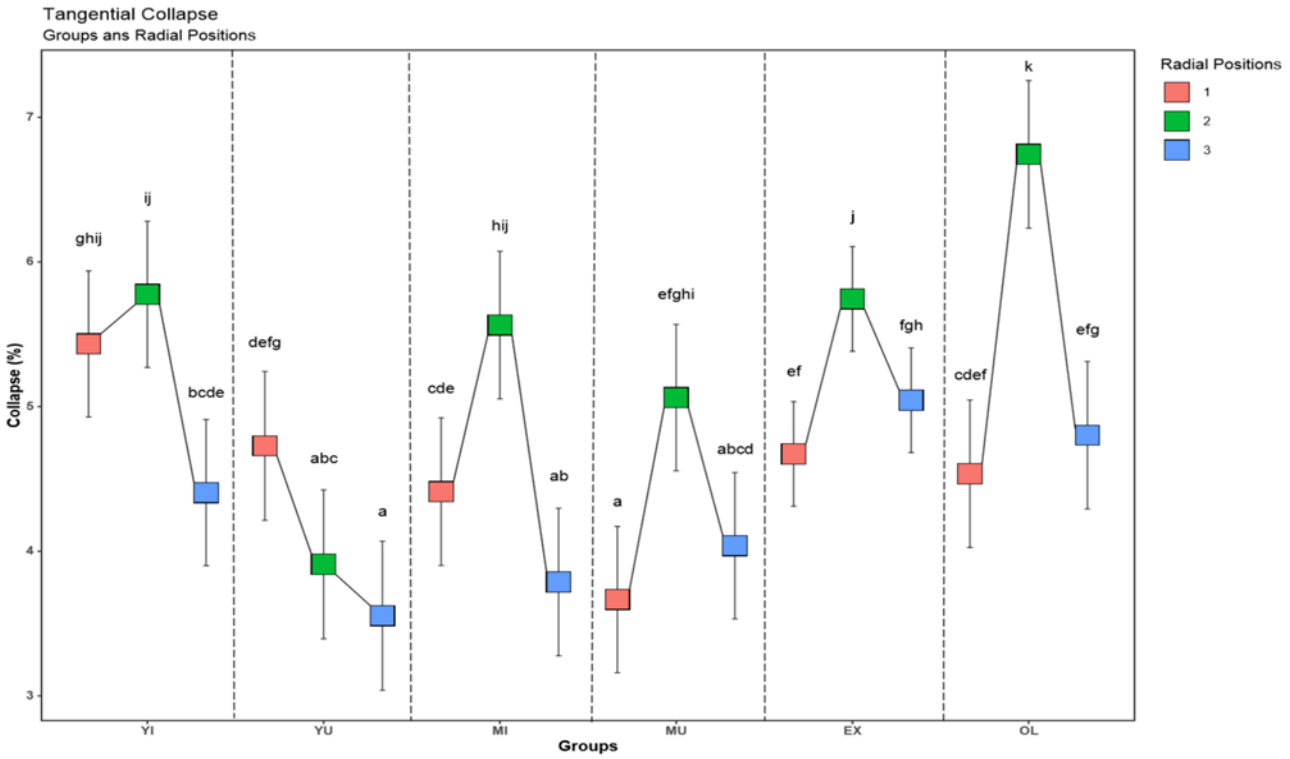

Figure 4- 11: The interaction between groups and radial positions for tangential collapse.

Figure 4-11 is roughly a mirror image of the trends observed with density measurements. This is supported by the significant correlation between density and collapse (*see Table 4.17* and *4.18*). The literature has reported woods of low to medium densities to be susceptible to collapse, suggesting a negative relationship between the two properties. Yang et al. (2018) reported high density wood inhibits collapse even in non-permeable woods as the cell walls are thick enough to withstand the capillary forces. Similar findings were reported by Ananías et al. (2014) where he used blocks to measure collapse representing three sections as they are in this study. He found that the transition zone (radial position 2) had at least 50% more collapse than the core and outer wood. Collapse also seem to increase with age with only the YI group not conforming to the trend. It seems like collapse was partly a function of density and the negative relationship between them.

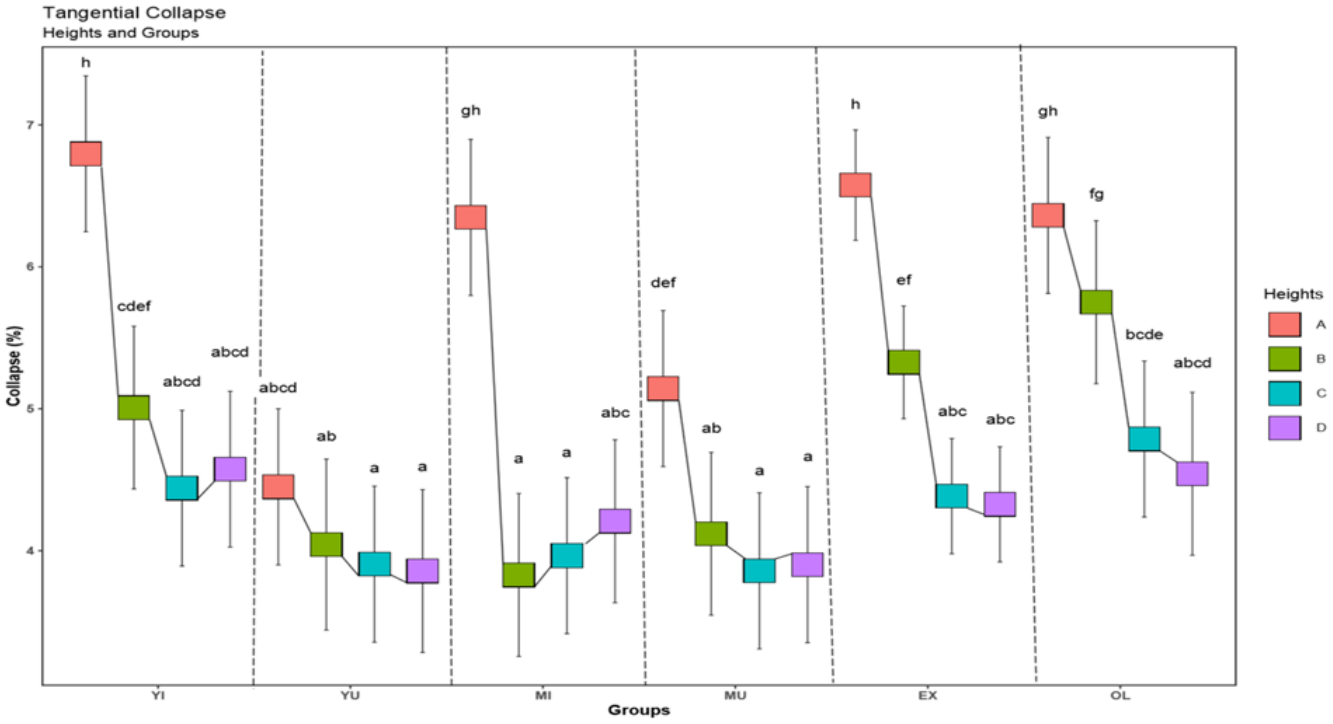

Figure 4- 12: The interaction between groups and heights for tangential collapse.

Figure 4-12 showed that the breast height tangential collapse was significantly higher than collapse at other heights for all the groups except the OL group. There was mostly no difference between collapse at other heights within a group except for the two older groups (EX and OL) where the B height also had significantly higher collapse than other samples. A similar trend was reported by others (Kauman 1960; Pankevicius 1961 in Priadi 2001) where collapse decreased from the stump height to the top of the tree. Another factor that might have played a role was the size of samples and the path of water movement out of the samples. Water movement out of the centre section of the wedges might have been more difficult since the distance in the radial and tangential directions to a surface is longer – leading to more cellular stress and collapse. The longitudinal distance will stay the same of course, since disk thickness was relatively constant at all positions. This hypothesis (of sample size, water movement) need to be tested in a different setup. It is also not clear why the radial and tangential collapse will have such a different profile (*see Figures 4-9, 4-11, 4-12*). According to the current results it seems as if collapse of cells occurred in the radial direction on the outer parts of the wedges (*Figure 4-9*) but in the tangential direction in the centre parts of the disks (*Figure 4-11*).

4.6.3 Collapse (boards)

The collapse data for boards was normally distributed and the lmer () function was used to model and analyse the data. *Table 4-8* shows that all main effects as well as first order interactions were significant.

Table 4- 8*:* The ANOVA table for collapse on the boards.

Collapse

	Random effects:				
	Groups Name	Variance	Std Dev		
	Tree Intercept	16.12	4.015		
	Residual	112.42	10.603		
Effect	DF	Sum Sq	Mean Sq	F-value	p-value
Log	1	1315.7	1315.69	11.7032	0.0007620
Radial Position	2	2428.7	1214.37	10.8020	5.849e-06
Group	5	4045.4	809.08	7.1969	8.123e-07
Log:RadialPosition	2	727.2	363.60	3.2343	0.0307417
Log:Group	5	2526.8	505.35	4.4952	0.0006581
RadialPosition:Group	10	2530.2	253.02	2.2507	0.0127216
Log:RadialPosition:Group	10	1413.2	141.32	1.2571	0.2486720

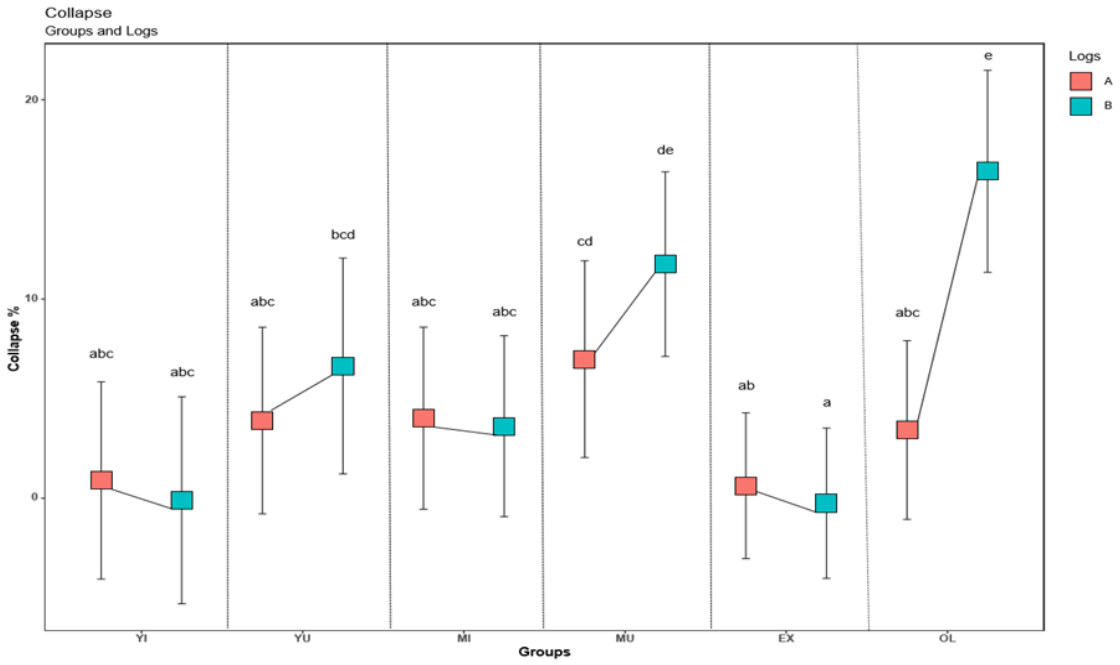

Figure 4- 13: The interaction between groups and logs for collapse on boards.

Figure 4-13 shows that there was no difference between log A (bottom log) and log B (top log) in all groups except group OL. There don't seem to be a large age effect either. The only difference worth mentioning is the increase of board collapse from log A to log B for the old group.

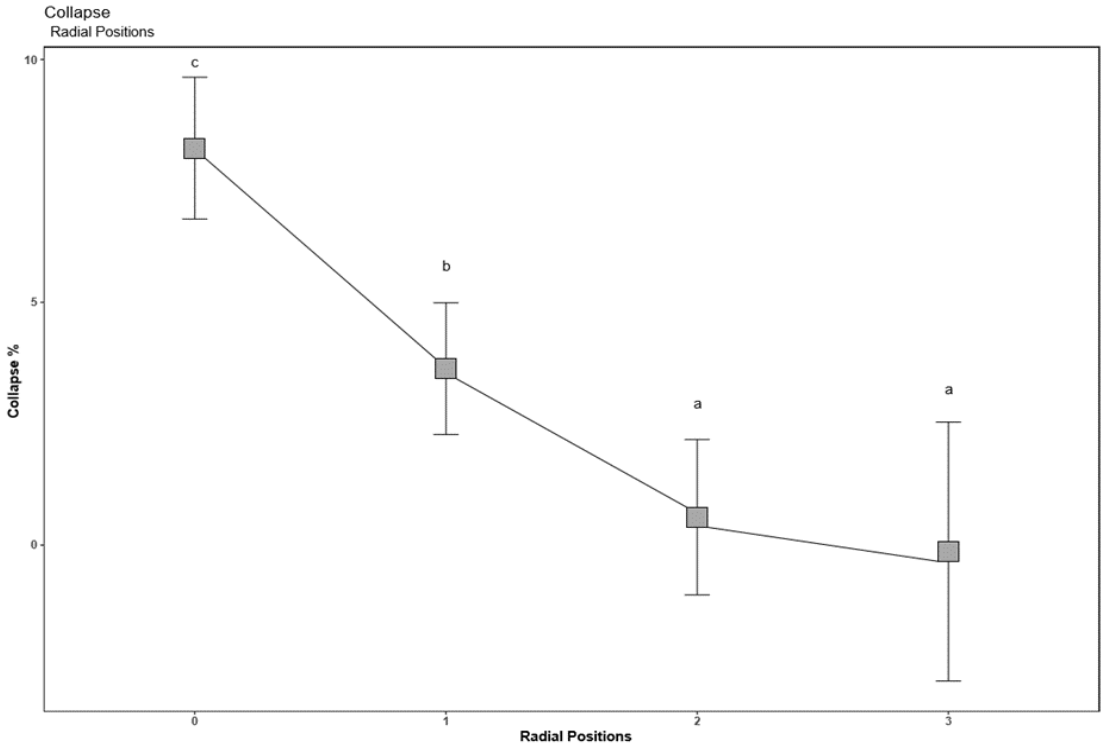

Figure 4- 14: The radial variation of collapse in boards.

Collapse in boards was based on a visual assessment of surface of the boards assigning the percentage based on the area of the surface showing collapse. *Figure 4-14* shows that collapse was the highest at the centre and gradually decreased and the boards at position 2 and 3 had virtually no collapse.

The results from this study posed some interesting questions around the measurement of collapse and the reasons for collapse. It seems as if collapse of cells occurred in the radial direction on the outer parts of the wedges but in the tangential direction in the centre parts of the wedges (*Figure 4-9 and 4-11*). Also, for the wedges, collapse was highest at breast height (*Figure 4-12*). On the boards, however, collapse was highest on the pith-boards and, for the old group (OL), it was highest in the top logs. This was the exact opposite collapse behaviour than that experienced on the wedges.

One reason for the difference between boards and discs samples might be due to the size and the fact that the centre boards combines wood from different radial zones (Priadi, 2001). Furthermore; the boards were dried in a kiln using the drying schedule that is used to dry commercial timber

hence, collapse recovery may have taken place. Ananías et al. (2014) reported the highest collapse recovery is at the transition zone, while the highest residual collapse is found near the pith. It is clear that a better understanding of collapse measurement is required – perhaps using another type of experimental setup.

4.7 Shrinkage

4.7.1 Samples (Radial)

The data for radial shrinkage was normally distributed and the lme () function was used to model and analyse the data. *Table 4-9* shows that all the effects were highly significant and the only interaction that was significant is that of radial position and group.

Table 4- 9*:* The ANOVA table for radial shrinkage.

Radial Shrinkage

Random effects: Formula: ~1 | Tree				
	Intercept	Residual		
Std Dev:	0.2968985	0.6181346		
Effect	numDF	denDF	F-value	p-value
Intercept	1	661	2669.2251	<.0001
Radial Position	2	661	98.0539	<.0001
Height	3	661	32.7827	<.0001
Group	5	64	13.3123	<.0001
RadialPosition:Height	6	661	1.9423	0.0718
RadialPosition:Group	10	661	4.5779	<.0001
Height:Group	15	661	1.3586	0.1619
RadialPosition:Height:Group	30	661	0.9165	0.5967

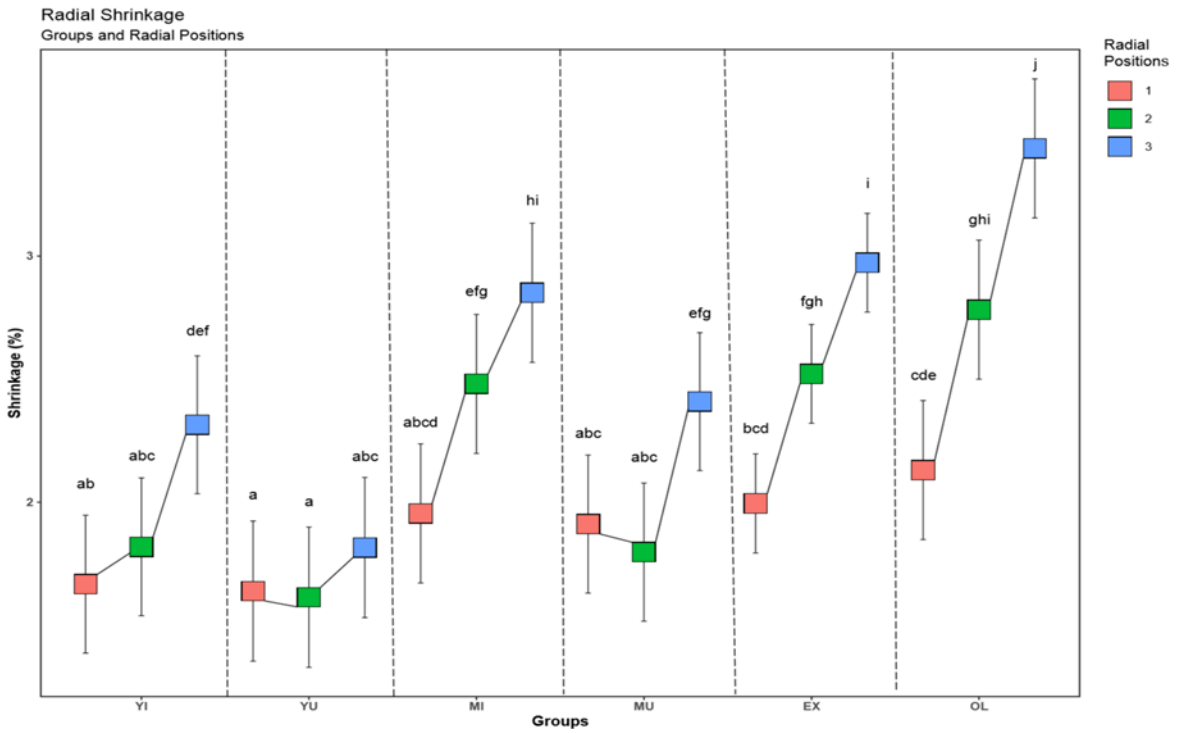

Figure 4- 15: The interaction of radial positions and groups for radial shrinkage.

Figure 4-15 shows radial shrinkage as linear function of radial position. Shrinkage increased consistently from radial position 1 to 3. *Figure 4-1 of section 4.1* showed that density is almost always the highest at position 3 and increased with age, the same is observed for shrinkage. The effect of age comes to light with old groups having slightly higher shrinkage compared to young and mature groups and a significant variation between radial position 3 observed from young to mature and old trees.

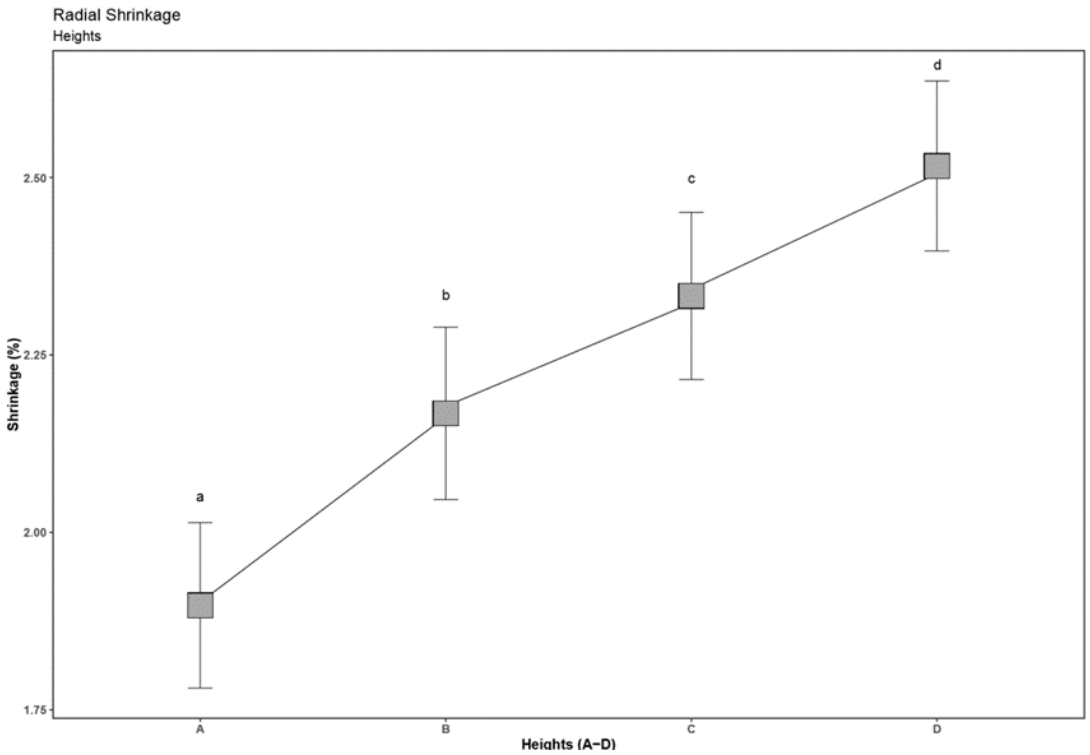

Figure 4- 16: The effect of height on radial shrinkage.

Figure 4-16 shows shrinkage increased consistently with height. Again, the same relationship observed for radial density variation holds for the height variation. All four heights were significantly different from each other ranging between 1.75%-2% from height A to about 2.5% at height D. These values were slightly lower compared to an average of 2.56% at breast height reported by Ananías et al. (2014) for radial shrinkage.

4.7.2 Samples (Tangential)

The data for tangential shrinkage was normally distributed and the lme () function was used to model and analyse the data. *Table 4-10* shows that all effects were highly significant and the only significant interaction was that of height and group. However, no firm conclusions could be drawn from the graph of the interaction. Hence, only the results for the main effects are displayed below.

Table 4- 10*:* The ANOVA table for tangential shrinkage.

Tangential Shrinkage

	Random effects: Formula: ~1 | Tree			
	Intercept	Residual		
Std Dev:	0.3679211	1.004327		
Effect	NumDF	denDF	F-value	p-value
Intercept	1	662	3102.3604	<.0001
Radial Position	2	662	25.6294	<.0001
Height	3	662	8.4695	<.0001
Group	5	64	10.9272	<.0001
RadialPosition:Height	6	662	0.6052	0.7263
RadialPosition:Group	10	662	1.3207	0.2151
Height:Group	15	662	1.8968	0.0208
RadialPosition:Height:Group	30	662	0.5301	0.9824

Figure 4-17 shows an increasing trend of tangential shrinkage and can be linked to density as well which also increased with age as discussed in section 4.1.

Figure 4-18 shows similar radial trends for tangential shrinkage as observed for radial shrinkage in section 4.7.1 with increasing shrinkage further from the pith.

Figure 4-19 shows the trend somewhat similar to the one observed for radial shrinkage in the previous section viz. increasing tangential shrinkage with height.

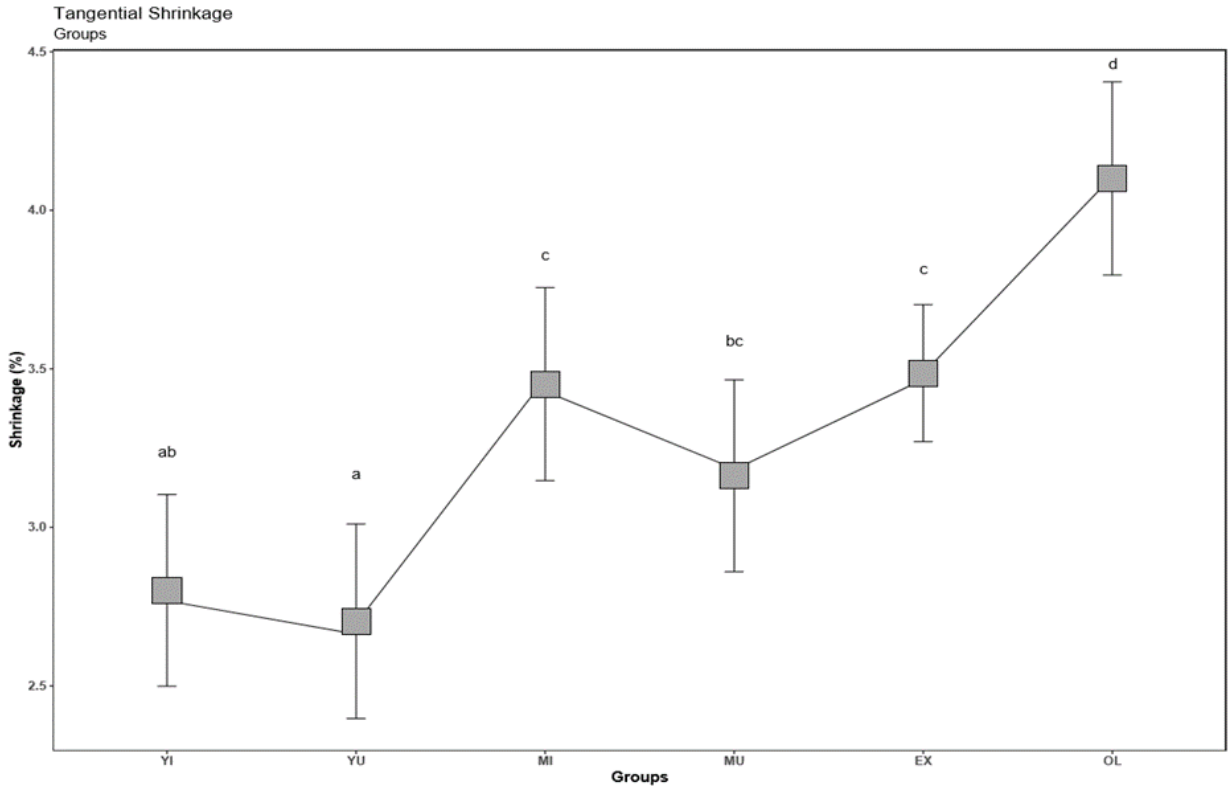

Figure 4- 17: The effect of groups on tangential shrinkage.

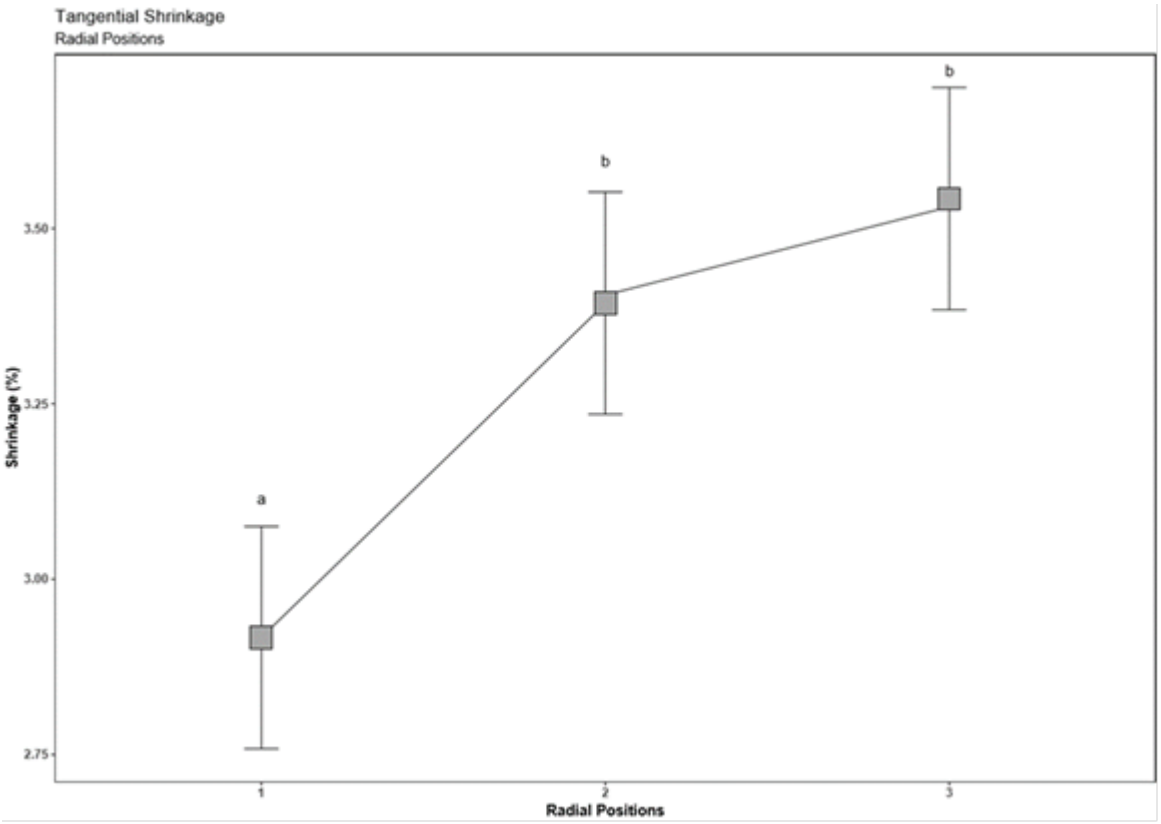

Figure 4- 18: The effect of radial positions on tangential shrinkage.

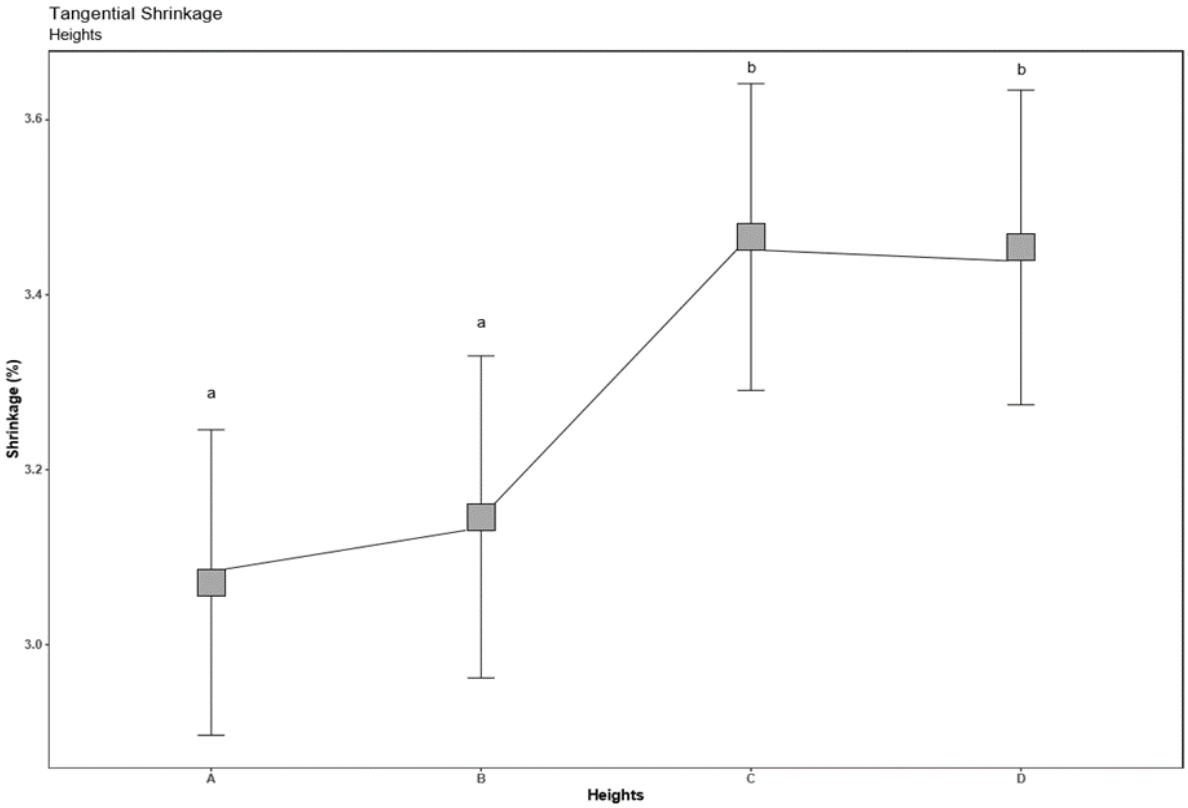

Figure 4- 19: The graph showing the effect of heights on tangential shrinkage.

4.7.3 Board shrinkage (thickness direction)

The data for shrinkage on boards was normally distributed and the lmer () function was used to model and analyse the data. *Table 4-11* shows that all the effects were highly significant and the interactions between log and group, and radial position and group were also highly significant. The graphs showing the interaction between log and group and the effect of radial position are displayed below:

Table 4- 11*:* The ANOVA table for Shrinkage (thickness) on boards.

Boards Shrinkage Thickness

Random effects:

Groups	Name	Variance	Std Dev
Tree	Intercept	0.4584	0.6771
Residual		1.4242	1.1934

Effect	DF	Sum Sq	Mean Sq	F-value	p-value
Log	1	29.737	29.737	20.8794	< 2.2e-16
Radial Position	2	92.324	46.162	32.4120	< 2.2e-16
Group	5	15.420	3.084	2.1654	< 2.2e-16
Log:RadialPosition	2	2.442	1.221	0.87572	0.6634
Log:Group	5	40.894	8.179	5.7426	5.308e-05
RadialPosition:Group	10	31.960	3.196	2.2440	0.01742
Log:RadialPosition:Group	10	8.662	0.866	0.6082	0.8129

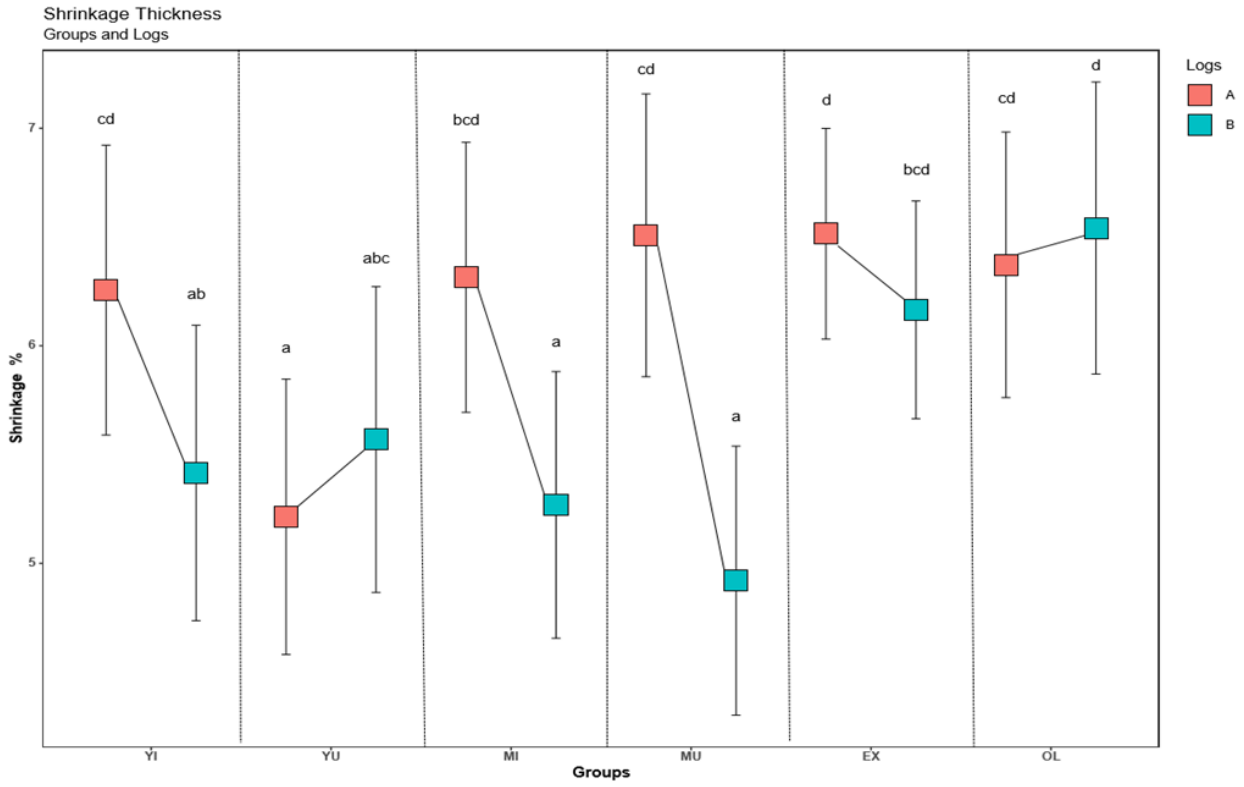

Figure 4- 20: The interaction between logs and groups for shrinkage (thickness) for boards.

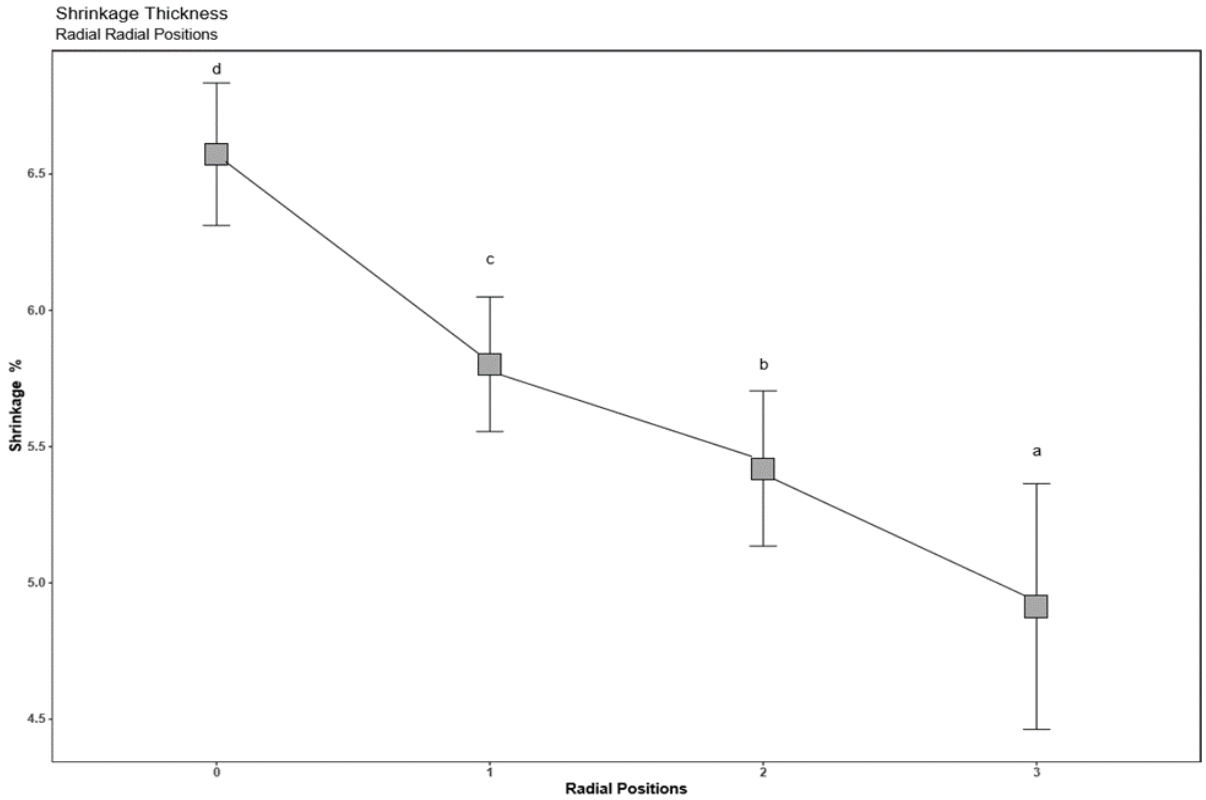

Figure 4- 21: The effect of radial position on shrinkage (thickness) for boards.

Figure 4-20 shows the interactions between logs and groups and *Figure 4-21* the effect of radial position in thickness shrinkage. The shrinkage on boards was again quite different to that experienced in the wedges. On the wedges shrinkage was always increasing with increasing height – for both radial and tangential shrinkage. On the boards in the thickness direction, however, three groups had significantly higher shrinkage on the bottom log and for three groups there were no significant differences between the bottom and top logs (*Figure 4-20*). On the wedges both radial and tangential shrinkage had an increasing trend from the pith to the outer wood. With the boards, however, there was a very consistent decreasing trend in thickness shrinkage from the pith towards the bark (*Figure 4-21*).

Findings by Kauman (1958) as reported in Priadi (2001) was similar where it was reported that no matter in what direction the wood was cut (radial or tangential) the total shrinkage and collapse was always the highest in the thickness direction and at the centre, while it was the lowest in the width direction.

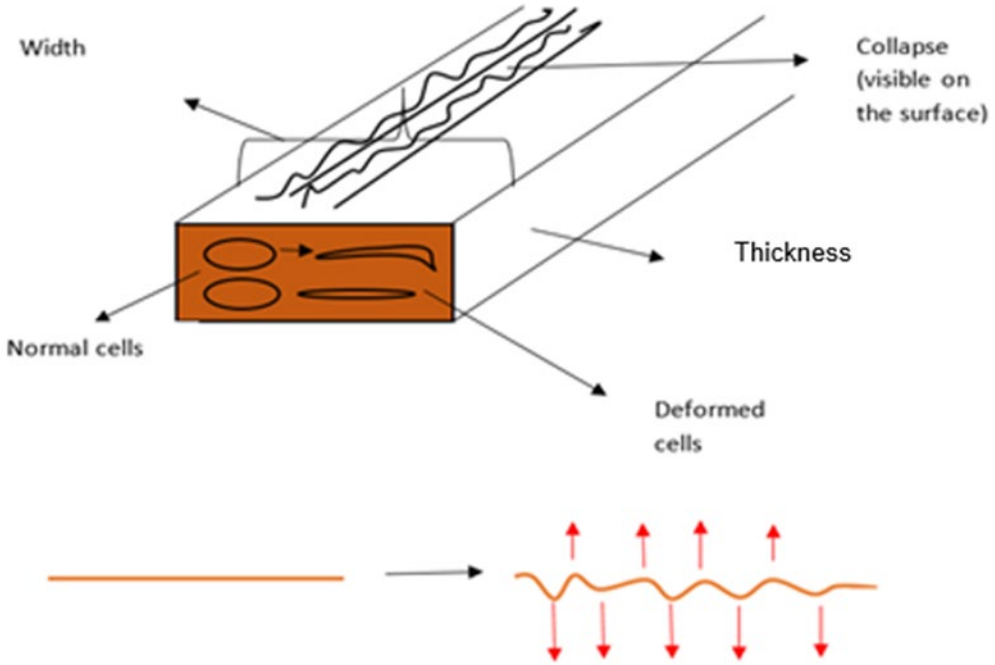

Figure 4- 22: The diagram that shows the flattening of the cells in boards during drying.

Kauman (1960) in Priadi (2001) explained that the bigger samples result in a larger amount of collapse due to the moisture gradient created during the drying of wood and the greatest size being in the width direction (*figure 4-22*). The cells flatten across the width direction resulting in high shrinkage in the thickness directions. As previously discussed in section 4.6 collapse is the highest at the centre boards and the shrinkage on boards for this study did not consider the collapse on boards. The difference in shrinkage behaviour in wedges compared to that of boards might therefore partly be due to collapse. For the wedges, the effect of collapse was removed from the shrinkage results, through a calculation (see Methods section).

4.7.4 Boards shrinkage (width direction)

The shrinkage data in the width direction was normally distributed and the lmer () function was used to model and analyse the data. *Table 4-12* shows that the main effects of radial position and group were highly significant, while log was not significant at all. The interactions between log and group, and radial position and group were also significant. Only the graph showing the interaction between radial position and group is displayed below:

Table 4- 12: The ANOVA table for shrinkage (width) boards.

Boards Shrinkage Width

	Random effects:				
	Groups Name	Variance	Std Dev		
	Tree Intercept)	0.4584	0.6771		
	Residual	1.4242	1.1934		
Effect	DF	Sum Sq	Mean Sq	F-value	p-value
Log	1	0.924	0.924	0.8643	0.85752
Radial Position	2	250.623	125.312	117.2204	< 2.2e-16
Group	5	37.381	7.476	6.9935	1.390e-06
Log:RadialPosition	2	1.140	0.570	0.5331	0.4712
Log:Group	5	15.828	3.166	2.9613	0.01526
RadialPosition:Group	10	47.933	4.793	4.4838	2.326e-06
Log:RadialPosition:Group	10	16.153	1.615	1.5110	0.1404

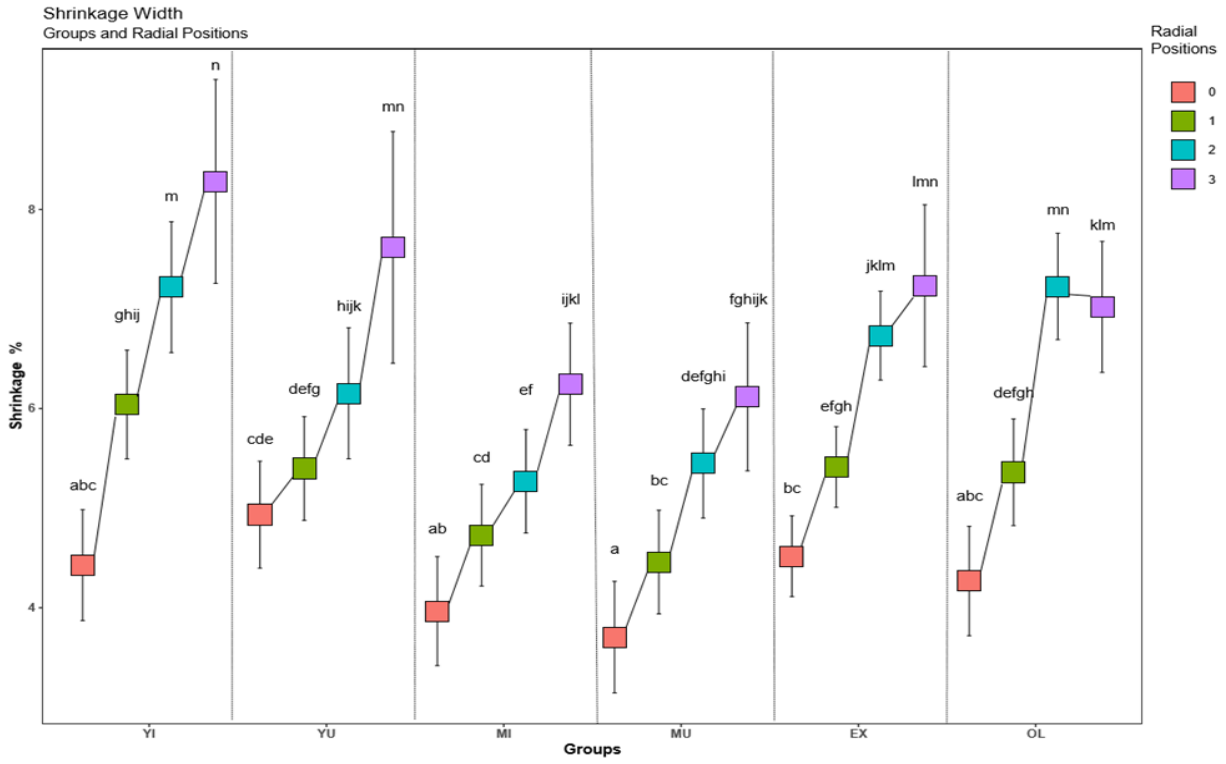

Figure 4- 23: The interaction between radial positions and groups for shrinkage (width) on boards.

Figure 4-23 shows a steady increase in width shrinkage from radial position 0 to radial position 3. This trend was similar to the results from the small wedges samples in this study. It is quite different to the thickness shrinkage experienced in boards – giving weight to the argument that thickness shrinkage was probably influenced by collapse.

4.8 Collapse free shrinkage

The collapse free shrinkage using ethanol to replace water in wood did not work very well, as the shrinkage obtained from them was not different from shrinkage obtained from samples that were not treated with ethanol. This could possibly be due to the fact that too many samples (315 wedges) were treated at the same time.

Table 4- 13: table showing the p-value for normality test and for the t-test of the two-measuring techniques.

Normality test		
Test	*Sample type*	*p-values*
Shapiro-wilk normality test	Radial shrinkage Blocks	0.3344
Shapiro-wilk normality test	Radial shrinkage Wedges	0.5291
Shapiro-wilk normality test	Tangential shrinkage Blocks	0.9506
Shapiro-wilk normality test	Tangential shrinkage Wedges	0.0154
Actual test		
Test	*Direction*	*p-value*
t.test	Radial shrinkage	0.6716
Wilcoxon rank sum test	Tangential shrinkage	0.3736

The data for wedges in the tangential direction was not normally distributed with p-value of 0.0154 which is less than 0.05, meaning that the null hypothesis that the data was normally distributed was rejected. The Wilcoxon Rank Sum test was used to analyse the data in the tangential direction and the results were the same with those obtained from t-test. *Table 4-11* shows the results of the comparisons between the two techniques (wedges and blocks). The p-value for radial shrinkage is greater than 0.05 (0.6716) meaning the null hypothesis cannot be rejected that the two means are the same. The two methods gave similar means of shrinkage (see *figure 4-24 A* for the means).

For tangential shrinkage however, the p-value was greater than 0.05 (0.3736) meaning the null hypothesis cannot be rejected. The two means were not significantly different from one another.

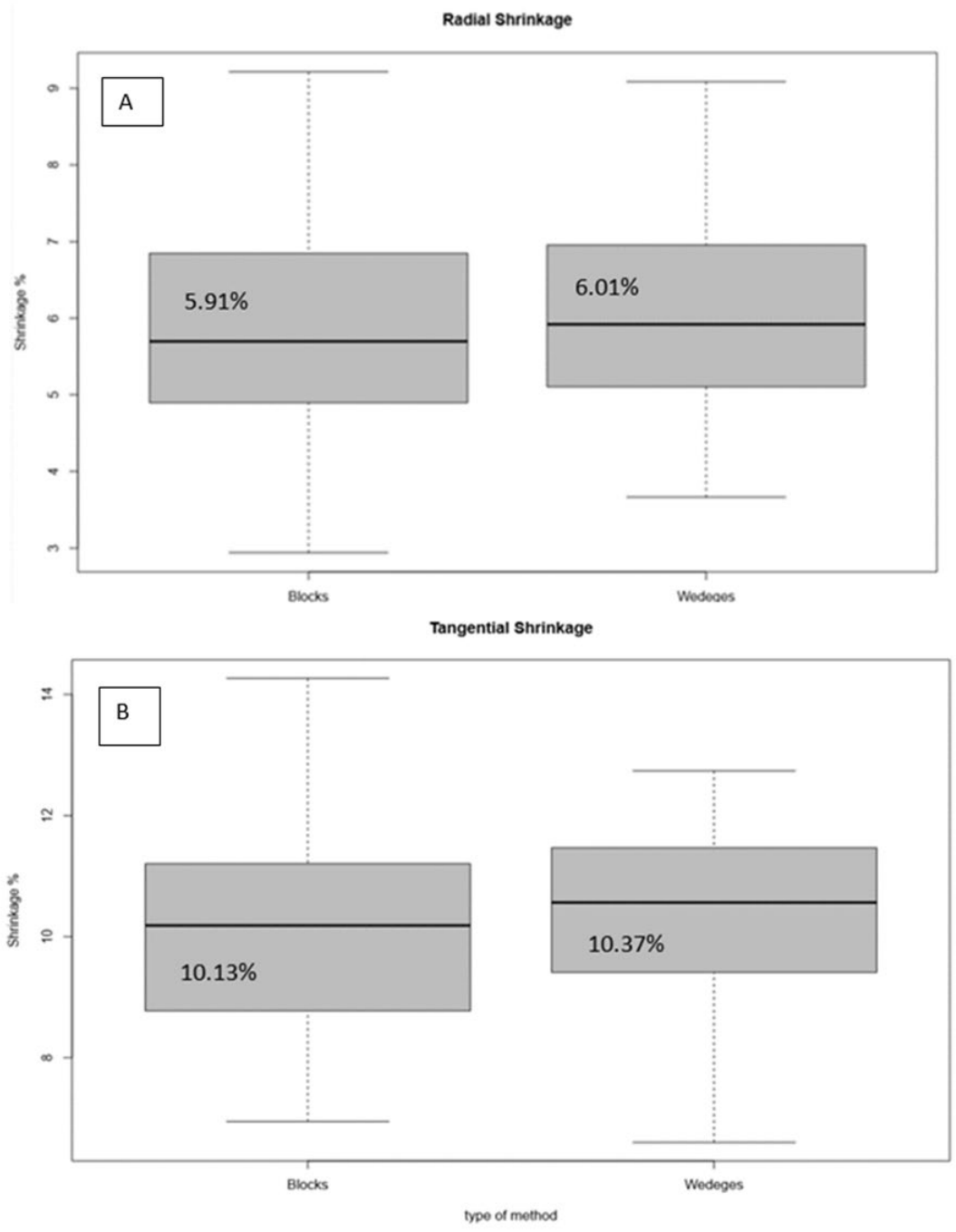

Figure 4- 24: Boxplots showing the means of wedges and blocks for (A) radial and (B) tangential shrinkage.

The two means can be seen in *figure 4-24 (B).* They are similar however; the wedges data was skewed to the left (below the mean).

4.9 Twist

The data for twist was normally distributed and the lmer () function was used to analyse the data. *Table 4-14* shows that only the main effect group was significant with regards to twist.

Table 4- 14*:* The ANOVA table for twist.

Twist

	Random effects:				
	Groups Name	Variance	Std Dev		
	Tree Intercept	0.01183	0.1088		
	Residual	0.13039	0.3611		
Effect	DF	Sum Sq	Mean Sq	F-value	p-value
Log	1	0.00064	0.00064	0.0049	0.99859
Radial Position	2	0.52842	0.26421	2.0263	0.08333
Group	5	1.84824	0.36965	2.8349	0.01639
Log:RadialPosition	2	0.27883	0.13942	1.0692	0.30440
Log:Group	5	0.91660	0.18332	1.4059	0.236246
RadialPosition:Group	10	2.29236	0.22924	1.7581	0.06246
Log:RadialPosition:Group	10	1.19199	0.11920	0.9142	0.51872

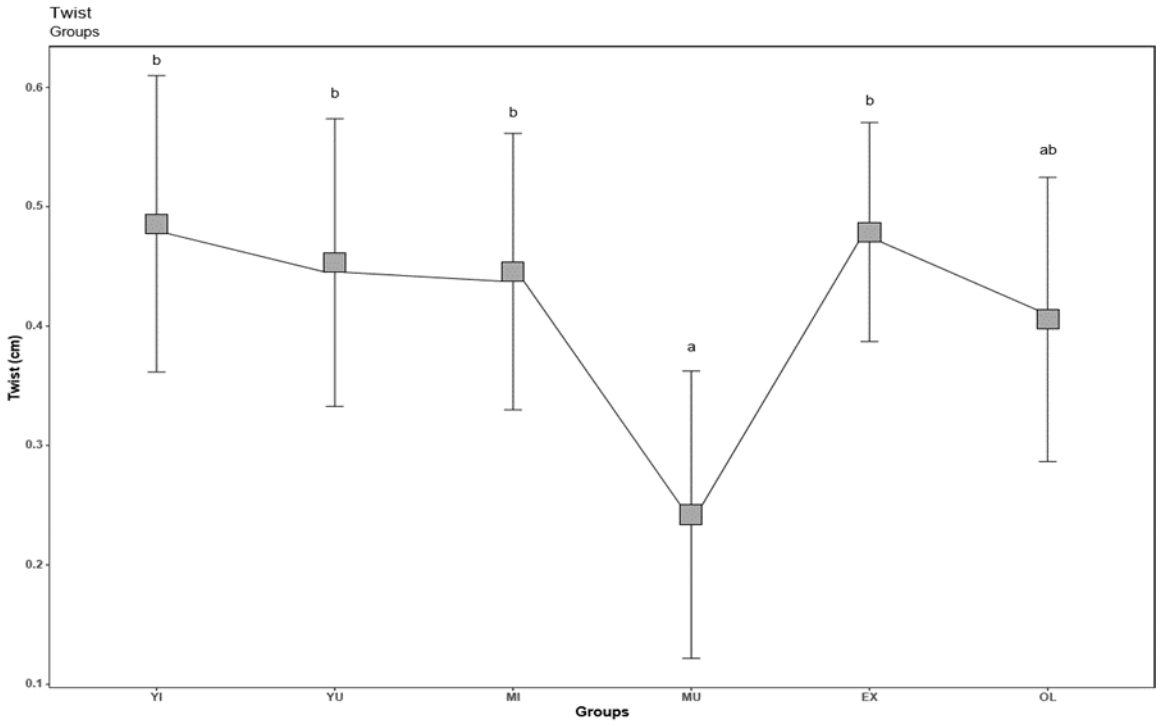

Figure 4- 25: The the effect of groups on twist.

Figure 4-25 shows no significant difference between all the groups except for the mature unimproved (MU) group which had slightly lower mean twist than other groups. Twist of boards varied between 1 mm and 6 mm and compared to the national standard requirement of 18 mm for

stress-graded structural timber and sawn *Eucalyptus* timber (SANS 1783-2. 2012; SANS 1707-1. 2010) the twist was much lower. For industrial lumber the SANS 1783-3 (2010) prescribes 2º and 18 mm is the equivalence of 9º making the samples in this study way lower than the industrial lumber requirements as well. This means that *Eucalyptus grandis* and *E. grandis X urophylla* would potentially pass as stress-graded timber and industrial lumber based on the results of twist observed.

4.10 Bow

The data for bow was normally distributed and the lmer () function was used to analyse the data. *Table 4-15* shows that the factors radial position and group were highly significant, also the interaction between radial position and group was significant. However, no firm conclusions could be drawn from the interaction as a result the graphs showing the two effects are shown below:

Table 4- 15*:* The ANOVA table for bow.

Bow (dry)

Groups	Name	Variance	Std Dev
Tree	Intercept	0.0	0.00
Residual		112.2	10.59

Effect	DF	Sum Sq	Mean Sq	F-value	p-value
Log	1	238.2	238.2	2.1239	0.13480
Radial Position	2	13590.0	6795.0	60.5808	<2e-16
Group	5	2482.8	496.6	4.4270	0.00052
Log:RadialPosition	2	148.6	74.3	0.6624	0.52043
Log:Group	5	638.3	127.7	1.1382	0.48157
RadialPosition:Group	10	2562.2	256.2	2.2843	0.01134
Log:RadialPosition:Group	10	819.1	81.9	0.7303	0.69661

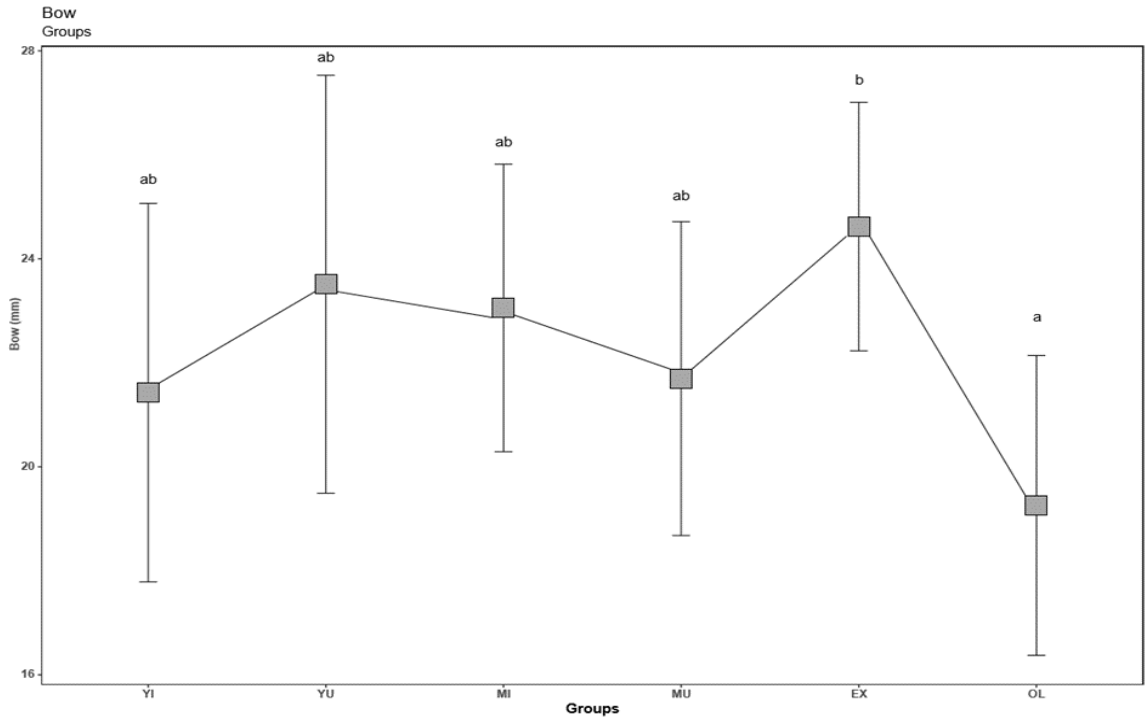

Figure 4- 26: The effect of groups on bow.

Figure 4-26 shows no significant difference between groups except between EX and OL – all the other groups were not significantly different from each other ranging between 16 mm – 28mm. The bow compared well with 10 mm per 1 m length piece prescribed by the SANS 1783-2 (2012). Bow in dried timber are often a result of variation in radial shrinkage over the cross-section of a log. It sometimes occurs when there is tension wood in the timber where large differences in micro fibril angle over the cross section are present.

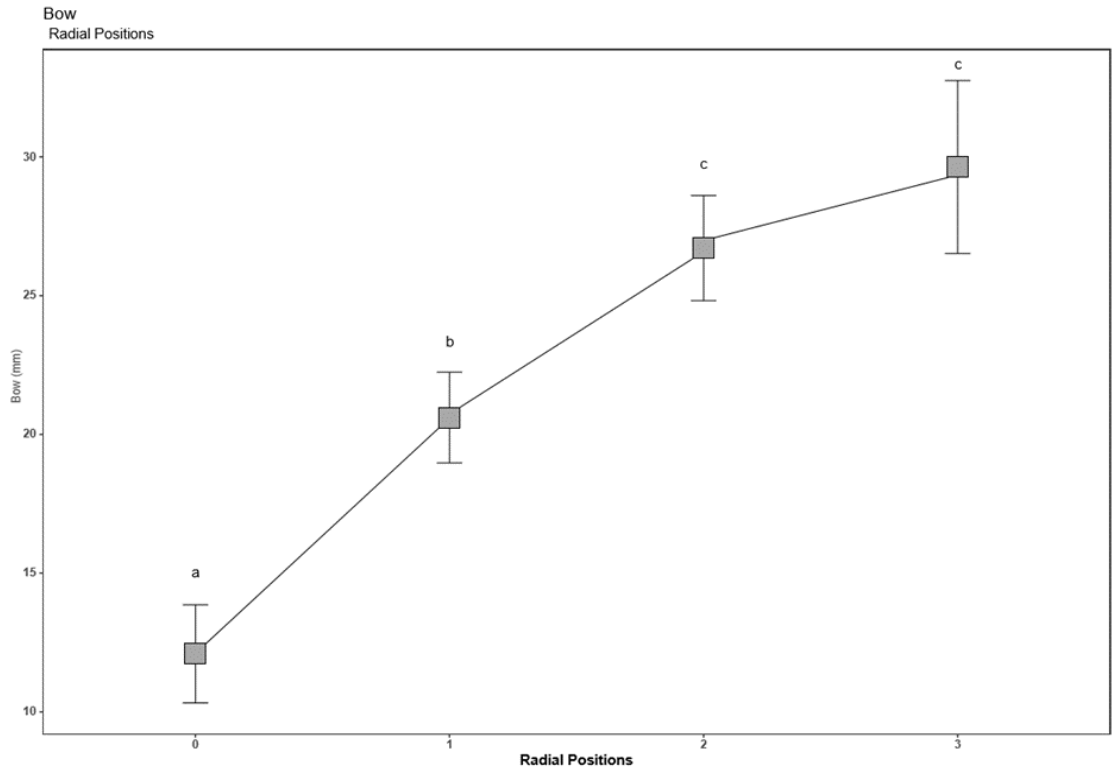

Figure 4- 27: The effect of radial positions on bow.

A maximum bow of 10 mm per 1 m length of piece is prescribed by the SANS 1707-1 (2012). The samples in this study were 4.2 m long giving them a maximum allowable bow of 40 mm (SANS 1783-2. 2012; SANS 1707-1. 2010). Bow was thus fairly low compared to allowable levels. *Figure 4-27* shows that bow increased from pith to bark like shrinkage – and differentials in radial shrinkage are probably the cause for most of the bow observed.

4.11 Cup

The data for cup was normally distributed and the lmer () function was used to analyse the data. It can be seen in *table 4-16* that all three effects were highly significant and only the interaction between radial group and group was significant. Nothing of substance could be concluded from the effect of log on cup hence, the graph displaying the interaction of radial position and group is shown below:

Table 4- 16*:* The ANOVA table for cup.

Cup

	Random effects:				
	Groups Name	Variance	Std Dev		
	Tree Intercept	0.0001362	0.01167		
	Residual	0.0130294	0.11415		
Effect	DF	Sum Sq	Mean Sq	F-value	p-value
Log	1	0.24297	0.242968	18.6477	9.182e-06
Radial Position	2	0.09388	0.046942	3.6028	0.028905
Group	5	0.21741	0.043482	3.3372	0.005052
Log:RadialPosition	2	0.00831	0.004156	0.3190	0.878231
Log:Group	5	0.05098	0.010197	0.7826	0.458727
RadialPosition:Group	10	0.38785	0.038785	2.9767	0.000935
Log:RadialPosition:Group	10	0.11624	0.011624	0.8922	0.539553

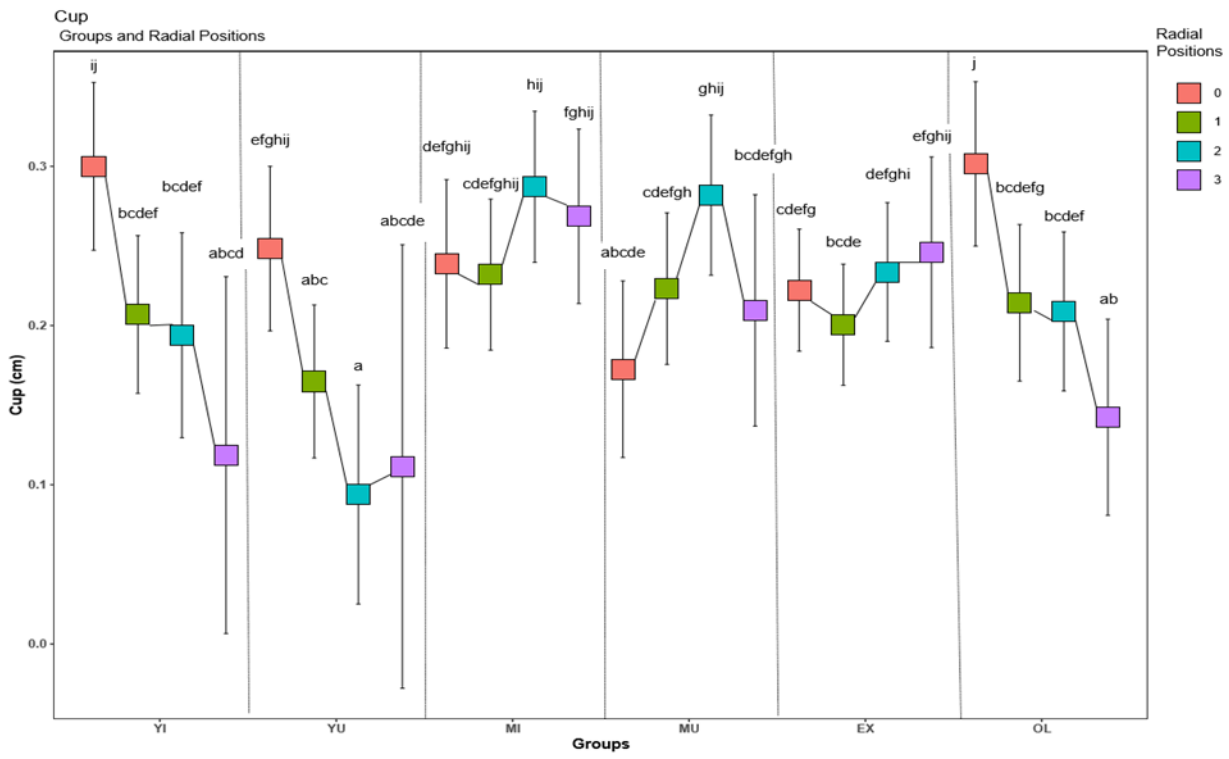

Figure 4- 28: The interaction between groups and radial positions for cup.

Cup for all the groups ranged from 0.0 cm (0 mm) to +0.3 cm (3 mm) which is comparable to the limit of 3 mm per 100 mm of width prescribed in the SANS 1707-1 (2010). Pagel (2019) reported a mean of 0.98 mm cup for laminated *E. grandis* and 1.27 mm for standard boards of *E. grandis*. The cup can also be related to differences in shrinkage and collapse over the cross section of a board. The trend observed in *figure 4-28* is inconsistent making it difficult to draw firm conclusions.

4.12 Correlations between measured properties

Table 4- 17*:* The table showing the correlations and p- values for the wedge samples at breast height only. Significant correlations at the 0.05 level are highlighted. (n values are shown on the lower part of the table).

Correlation with Extractives content (only 1 height)	Correlation value *(p-value)*								
	Radial Shrinkage	Tangential Shrinkage	Radial Collapse	Tangential Collapse	Extractives contents	Density	MC	Permeability	H/S Ratio
Radial Shrinkage	1.00	0.49 *(0.0000)*	0.36 *(0. 0002)*	0.01 *(0. 9343)*	0.37 *(0. 0002)*	0.31 *(0. 0061)*	-0.19 *(0. 0612)*	-0.20 *(0. 0396)*	0.18 *(0. 0704)*
Tangential Shrinkage	102	1.00	0.14 *(0. 1685)*	-0.11 *(0. 2674)*	0.27 *(0. 0067)*	0.24 *(0. 0405)*	-0.22 *(0. 0249)*	-0.23 *(0. 0201)*	0.26 *(0. 0097)*
Radial Collapse	102	102	1.00	0.16 *(0. 0984)*	0.25 *(0. 0102)*	0.23 *(0. 0503)*	-0.06 *(0. 5257)*	-0.19 *(0. 0497)*	0.20 *(0. 0456)*
Tangential Collapse	102	102	102	1.00	-0.10 *(0. 3408)*	-0.29 *(0. 0105)*	0.19 *(0. 0551)*	-0.13 *(0. 1975)*	0.15 *(0. 1219)*
Extractives contents	102	102	102	102	1.00	0.31 *(0. 0061)*	-0.06 *(0. 5491)*	-0.13 *(0. 2013)*	0.00 *(0. 9753)*
Density	76	76	76	76	76	1.00	-0.20 *(0. 0767)*	-0.15 *(0. 1901)*	-0.01 *(0. 9037)*
MC	102	102	102	102	102	76	1.00	0.22 *(0. 0271)*	-0.19 *(0. 0571)*
Permeability	102	102	102	102	102	76	102	1.00	-0.18 *(0. 0705)*
H/S Ratio	102	102	102	102	102	76	102	102	1.00

Table 4- 18*:* The table showing correlations and p-values for properties measured on wedge samples at all heights. Significant correlations at the 0.05 level are highlighted. Extractives content is not included here since it was only measured at breast height. (n values are shown on the lower part of the table.

Correlation without Extractives (All Heights included)	Correlation value *(p-value)*							
	Radial Collapse	Tangential Collapse	Radial Shrinkage	Tangential Shrinkage	Density	MC	Permeability	H/S Ratio
Radial Collapse	1.00	0.31 *(0.0000)*	0.20 *(0.0000)*	0.19 *(0.0000)*	0.22 *(0.0000)*	-0.07 *(0.0375)*	-0.15 *(0.0000)*	0.29 *(0.0000)*
Tangential Collapse	798	1.00	-0.05 *(0.1361)*	-0.20 *(0.0000)*	-0.02 *(0.5713)*	0.22 *(0.0000)*	-0.05 *(0.1515)*	0.30 *(0.0000)*
Radial Shrinkage	797	797	1.00	0.46 *(0.0000)*	0.29 *(0.0000)*	-0.46 *(0.0000)*	-0.22 *(0.0000)*	0.14 *(0.0001)*
Tangential Shrinkage	798	798	797	1.00	0.17 *(0.0000)*	-0.30 *(0.0000)*	-0.14 *(0.0001)*	0.13 *(0.0002)*
Density	558	558	558	558	1.00	-0.20 *(0.0000)*	-0.33 *(0.0000)*	0.02 *(0.6131)*
MC	781	781	780	781	563	1.00	0.16 *(0.0000)*	-0.11 *(0.0031)*
Permeability	747	747	746	747	536	758	1.00	-0.11 *(0.0018)*
H/S Ratio	780	780	779	780	549	778	751	1.00

Table 4- 19*:* The table showing the correlations and p-values for the properties measured on boards. Significant correlations at the 0.05 level are highlighted. (n values are shown on the lower part of the table).

Boards	Correlation value *(p-value)*						
	Shrinkage Width	Shrinkage Thickness	Bow (green)	Bow (dry)	Twist	Cup	Collapse
Shrinkage Width	1.00	0.09 *(0.0079)*	0.26 *(0.0000)*	*0.22* *(0.0000)*	0.09 *(0.0087)*	-0.05 *(0.1707)*	0.00 *(0.9473)*
Shrinkage Thickness	783	1.00	-0.23 *(0.0000)*	-0.17 *(0.0000)*	-0.05 *(0.1537)*	0.11 *(0.0011)*	0.01 *(0.7081)*
Bow (green)	820	865	1.00	0.45 *(0.0000)*	0.06 *(0.0750)*	-0.17 *(0.0000)*	-0.06 *(0.0512)*
Bow (dry)	814	859	934	1.00	0.14 *(0.0000)*	0.05 *(0.1160)*	-0.05 *(0.1449)*
Twist	816	862	943	931	1.00	0.07 *(0.0283)*	0.00 *(0.8908)*
Cup	816	862	937	932	934	1.00	0.04 *(0.2224)*
Collapse	817	861	943	932	940	934	1.00

Table 4-17 shows the correlations for the properties measured on disks and only at breast height. That was because extractives content was only measured at breast height. *Table 4-18* shows correlations between the same properties, but for disks measured at all heights and excludes extractives content. *Table 4-19* shows the correlations between properties measured on boards.

Collapse

As mentioned in the previous sections, it seems as if collapse of cells occurred in the radial direction on the outer parts of the wedges (sapwood) but in the tangential direction in the centre parts of the wedges (transition zone). Since the collapse behaviour also might have been influenced by the wedge geometry it is no surprise that correlations between collapse and other properties were relatively weak. At breast height radial collapse was significantly correlated to extractives content (r = 0.25) but tangential collapse was not correlated to extractives content at all (*Table 4-17*). The properties that were expected to influence collapse such as density, permeability, and extractives content did have a significant correlation with radial collapse (*Table 4-17 and Table 4-18*). Density and permeability did not have a significant relationship with tangential

collapse (*Table 4-18*). A very interesting result is the weak correlation between radial and tangential collapse (r = 0.31). This shows the clear directional nature of cell collapse. For future studies on collapse the following should be considered (1) sample geometry should be symmetrical, and (2) a combined radial/tangential collapse index should be considered. Also, board collapse behaved completely different to collapse in the wedge samples – which was probably a function of sample geometry and possibly collapse recovery that occur during the commercial drying schedule. Since the occurrence of collapse in sawn boards is of commercial importance, collapse measurements on smaller samples such as wedges should try to simulate what is happening in full sized sawn boards.

Shrinkage

As mentioned in the previous sections, it seems as if shrinkage was higher on the outer part (sapwood) of the wedges and it was lower in centre parts (heartwood) both in radial and tangential directions. Shrinkage was expected to correlate very well with extractives contents and density and at breast height shrinkage in both directions (radial and tangential) was significantly but weakly correlated to both extractives' contents and density with (r = 0.37 and r =0.31) and (r = 0.24 and r = 0.27) respectively (*see table 4-17*). Shrinkage also had a significant negative correlation with permeability and moisture content (r = -0.23 and r = -0.22) for both directions (*see table 4-17*). The positive significant correlation with heartwood/sapwood ratio (r = 0.26) was also observed (*see table 4-17*). Similar correlations were also observed with all four heights included; it is interesting to point a slight decline in correlation with density (r = 0.29 and r = 0.17) for both directions (*see table 4-17 and 4-18*). Also, quite notable is that correlations in radial directions were a bit higher compared to the ones in tangential directions (*table 4-17*). The positive relationship between density and extractives contents was not expected as extractives should result in less shrinkage but, this may possibly be due to the fact that only hot water extractives were considered.

Shrinkage in boards behaved different between width and thickness directions. Width direction follow the same trend as the wedge samples with higher shrinkage occurring on the outer boards. While in the thickness direction more shrinkage was observed in the centre boards and less shrinkage on outer boards, - but this was probably due to the influence of collapse on this direction as explained in section 4.7.3.

Warp

Bow had a trend similar to that of shrinkage (width) and a positive significant correlation (r = 0.26 and r = 0.22) for both bow green and bow dry respectively was observed (*see table 4-19*). The correlation between shrinkage (thickness) and bow was negative (r = -0.23 and r = -0.17) for bow green and bow dry respectively (*see table 4-19*). Cup did not have a conclusive trend as shown in

previous sections and did not show any correlations of interest with shrinkage. Both twist and cup showed variations between groups.

4.13 Multiple linear regression models

Multiple linear regression models were developed for both collapse and shrinkage (radial and tangential). Almost all the resulting models had significant p-values however, the r-squared values were very low. A number of models were developed (*Table 4-20 to Table 4-23*). However, these were of little practical value for predictions or even to get a better understanding of collapse and shrinkage behaviour due to the low coefficients of determination.

Table 4- 20*:* The table showing the p-values and r-squared values for radial collapse multiple linear regression. The highlighted section is the combination of the properties that resulted the best model.

Radial Collapse~		
Effect	*P-value*	*Adjusted R-squared*
Density + MC + Permeability + H/S Ratio + Extractives Contents	0.0126	0.1256
Extractives Contents + Permeability + H/S Ratio + MC	0.004341	0.1082
Extractives Contents + H/S Ratio + MC	0.003219	0.104
Extractives Contents + H/S Ratio	0.001068	0.1115

Table 4- 21*:* The table showing the p-values and r-squared values for tangential collapse multiple linear regression. The highlighted section is the combination of the properties that resulted in the best model.

Tangential Collapse~		
Effect	*P-value*	*Adjusted R-squared*
Density + MC + Permeability + H/S Ratio	5.026e-12	0.1022
MC + Permeability + H/S Ratio	< 2.2e-16	0.1441
MC + H/S Ratio	< 2.2e-16	0.153

Table 4- 22*:* The table showing the p-values and r-squared values for radial shrinkage multiple linear regression. The highlighted section is combination of the properties that resulted a better model.

Radial Shrinkage~		
Effect	*P-value*	*Adjusted R-squared*
Density + MC + Permeability + H/S Ratio	< 2.2e-16	0.2693
Density + MC + H/S Ratio	< 2.2e-16	0.252
Density + MC	< 2.2e-16	0.2519

Table 4- 23*:* The table showing the p-values and r-squared values for tangential shrinkage multiple linear regression models. The highlighted section is combination of the properties that resulted a better model.

Tangential Shrinkage~		
Effect	*P-value*	*Adjusted R-squared*
Density + MC + Permeability + H/S Ratio + Extractives Contents	0.02823	0.1008
Density + MC + Permeability + H/S Ratio	0.01347	0.1132
MC + Permeability + H/S Ratio	0.01319	0.0759
MC + Permeability	0.0102	0.07006

Chapter 5: Conclusions and recommendations

The objectives of the study were to profile the variations of collapse and shrinkage radially and along the height of trees and to explore the relationships they have with basic physical properties of the tree. The hypothesis was that the non-uniform dimensional changes found in the end products of *Eucalyptus grandis* are due to these variations.

An important finding in this study was that the properties measured on small wedge samples differed significantly from what was observed on sawn boards. This was true for both collapse and shrinkage - the properties on which this study focussed. In terms of the objectives of this study, the results on boards can be considered the most important. The results from the wedges does not really have commercial value attached to them and especially if they cannot be related to industrial sized boards like collapse did their application so far might be of importance for breeding to see which groups performed better in what properties i.e. group YU had the lowest collapse and shrinkage.

On boards, collapse varied depending on group, log position and the radial position of the boards. The radial position of the boards had a highly significant effect on board collapse, with collapse generally decreasing from pith to bark. There were first order interactions between all the factors and board collapse behaviour was not consistent throughout groups and log positions. In terms of the causal factors, there were weak but significant correlations between collapse and extractives content, density, and permeability (although these results should be viewed with caution since it was obtained from the small wedge samples). A very interesting result is the weak correlation between radial and tangential collapse on small wedge samples showing the clear directional nature of collapse.

On boards shrinkage varied depending on group, log position and the radial position of the boards. In the thickness direction shrinkage was higher in the centre boards and decreased towards the outer boards. This was due to the effect of collapse on the thickness direction as collapse is very size sensitive and no matter the direction (radial or tangential) the wider side experiences the most collapse. In the width direction, the shrinkage followed the normal pattern increasing from centre boards towards the outer boards. The width direction shrinkage had almost similar trends with the results found on wedges in both directions (radial and tangential).

Twist, bow and cup also varied significantly radially and along the height. However, the magnitude of these were generally far better than the requirements of national standards. Bow had a similar trend as shrinkage in the width direction. The trends for twist and cup were not consistent.

Some of the results obtained from small disk samples were inconclusive and contradicted what was observed in boards. It is recommended that future studies focus on obtaining a better understanding on the effect of specimen size. Although trends observed from the small samples were interesting, the practical significance is limited if the results cannot be related to observations in industrial size boards.

6. Reference List

Ahmed, S.A., Chun, S.K. 2011. PermeabiltyPermeability of *Tectona grandis* L. as affected by wood structure. *Wood Science Technology*, 45: 487-500.

Akbari, A., Hill, R.J., van de Ven, T.G.M., 2015. An elastocapillaryelectrocapillary model of wood-fibre collapse. *The Royal Society*, Available [rspa.royalsocietypublishing.org Proc.R.Soc.AProc.R. Soc.A471:20150184] 21] 21 November 2019.

Ananías, R.A., Sepúlveda-Villarroel, V., Pérez-Peña, N., Leandro-Zuñiga, L., Salvo-Sepúlveda, L., Salinas-Lira, C., Cloutier, A. and Elustondo, D.M. 2014. Collapse of *Eucalyptus nitens* wood after drying depending on the radial location within the stem. *Drying Technology*, 32(14), pp.1699–1705.

Bariska, M. 1992. Collapse phenomena in Eucalypts. *Wood Science and Technology*, 26: 165-179.

Bhat, K.M., Bhat, K.V., Dhamodaran, T.K. 1990. Wood density and fiber length of *Eucalyptus grandis* grown in Kerala, India. *Wood and Fiber Science*, 22(1): 54-61.

Bossu, J., Beauchêne, J., Estevez, J.Y., Duplais, C., Clair, B. New insights on wood dimensional stability influenced by secondary metabolites: The case of fast-growing Tropical species Bagassa guinanensis Aubli. *PLOS ONE*. Available [DOI: 10.1371/journal.pone.0150777] Accesed on 04 December 2019.

Carl, C., and Wiedenhoeft, A.C. 2009. Moisture-related properties of wood and the effects of moisture on wood and wood products. Research Gate. *Moisture Control In Buildings: The Key Factor in Mold Prevention,* 2: 54-79.

Chafe, S.C., Illic, J. 1992. Shrinkage and collapse in thin sections and blocks of Tasmanian ash regrowth. *Wood Science and Technology*, 25(5):343-351.

Chamberlain, D., Essop, H., Hougaard, C., Malherbe, S. and Walker, R. 2005. Part I: *The contribution, costs and development opportunities of the Forestry, Timber, Pulp and Paper industries in South Africa.* Final report – 29 June 2005. Johannesburg: Genesis Analytics (Pty) Ltd.

Cherelli, S.G., Sartori, M.M.P., Prospero, A.G., Ballarin, A.W. 2018. Heartwood and sapwood in Eucalyptus trees: non-conventional approach to wood quality. *Anais da Academia Brasileira de Ciências*, 90(1): 425-438.

Crafford, P.L. and Wessels, C.B. (2016). *The potential of young, green finger-jointed Eucalyptus grandis lumber for roof truss manufacturing. Southern Forests Journal*, 78(1): 60-71.

Crickmay and Associates. 2005. *Study of supply and demand of industrial roundwood in South Africa.* Hilton: Crickmay and Associates (Pty) Ltd.

Da Silva, M.R., Machado, G.O., Deiner, J., Junior, C.C. 2010. Permeability measurement of Brazilian *Eucalyptus*. *Materials Research*, 13(3): 281-286.

du Plessis, A., Meincken, M. and Seifert, T. (2013). Quantitative Determination of Density and Mass of Polymeric Materials Using Microfocus Computed Tomography. *Journal of Nondestructive Evaluation*, 32: 413–417.

Emaminasab, M., Tarmian, A. and Pourtahmasi, K. (2015). Permeability of poplar normal wood and tension wood bio-incised by Physisporinus vitreus and Xylaria longipes. *International Biodeterioration & Biodegradation*, 105: 178-184.

Engelund, E.T. 2011. Wood-water interactions linking molecular level mechanisms with macroscopic performance. *Technical University of Denmark*. PhD thesis.

Engelund, E.T., Thygesen, L.G., Svensson, S., Hill, C.A.S. 2013. A critical discdiskussion of the physics of wood-water interactions. *Wood Science Technology*, 47: 141-161.

Evans, A.A., Spagnolie, S.E., Bartolo, D., Lauga, E. 2018, *Elastocapillary self-folding, and collapse of floating filaments*. Available online [arXiv:1209.2149v1 [cond-mat.soft] 10 Sep 2012] 15 November 2019.

Freyburger, C., Longuetaud, F., Mothe, F., Constant, T. and Leban, J.-M. 2009. Measuring wood density by means of X-ray computer tomography. *Annals of Forest Science*, 66(8): 804–804.

Githiomi, J.K. and Dougal, E. 2012. Analysis of heartwood-sapwood dermacation methods and variation of sapwood and heartwood within and between 15-year-old plantation grown Eucalyptus regnans. *International Journal of Applied Science and Technology*, 2(8): 63-70.

Githiomi, J.K., Kariuki, J.G., 2010. Wood basic density of *Eucalyptus grandis* from plantations in central Rift valley, Kenya: variation with age, height level and between sapwood and heartwood. *Journal of Tropical Forest Science*, 22(3): 281-286.

Gominho, J., Pereira, H. 2005. The influence of tree spacing in heartwood content in *Eucalyptus globulus labill*. *Wood and Fiber Science*, 37(4): 582-590.

Hein, P.R.G., Siva, J.R.M., Brancheriau, L. 2013. Correlations among microfibril angle, density, modulus of elasticity, modulus of rapture and shrinkage in 6-year-old *Eucalyptus urophylla x E. grandis*. *Maderas. Ciercia Y Technologia*, 15(1): 171-182.

Jacobs MR. 1955. Growth habits of the Eucalypts. *Commonwealth Forestry and Timber Bureau, Canberra*.

Jakes, J.E., Hunt, C.G., Zelinka, S.L., Ciesielski, P.N. and Plaza, N.Z. 2019. Effects of Moisture on Diffusion in Unmodified Wood Cell Walls: A Phenomenological Polymer Science Approach. *Forests*, [online] 10(12): 1084. Available at: https://res.mdpi.com/d_attachment/forests/forests-10-01084/article_deploy/forests-10-01084.pdf [Accessed 5 Dec. 2019].

Kadas, M., 2016. *Greyscale-density calibration of an industrial CT scanner for wood mocrodensitometry.* Stellenbosch University. MSc thesis, Available [https://scholar.sun.ac.za] 16 November 2019.

Kumar, A., Dhillon, G.P.S., 2014. Variation of sapwood and heartwood content in half-sib properties of Eucalyptus tereticornis Sm. *Indian Journal of Natural Products and Resources*, 5(4): 338-344.

Leggate, W., Redman, A., Wood, J., Bailleres, H., Lee, D. 2019. Radial permeability of the hybrid Pine (Pinus elliottii x Pinus caribaea) in Australia. *BioResources*, 14(2): 4358-4372.

Malan FS. 1984. Studies on the phenotypic variation in growth stress intensity and its association with tree and wood properties of South African grown *Eucalyptus grandis* (Hill ex Maiden). Dissertation, University of Stellenbosch.

Malan FS. 1993. The wood properties and qualities of three South African-grown eucalypt hybrids. *South African Forestry Journal*, 167:35–44.

Malan FS. 2003. The wood quality of the South African timber resource for high-value solid wood products and its role in sustainable forestry. *South African Forestry Journal*, 198: 53–62.

Miranda, I. and Pereira, H. 2016. Variation of wood and bark density and production in coppiced *Eucalyptus globulus* trees in a second rotation. *iForest - Biogeosciences and Forestry*, 9(2): 270–275.

Miranda, I., Sousa, V., Pereira, H. 2011. Wood properties of teak (Tectona grandis) from a mature unmanaged stand in East Timor. *Journal of Wood Science.*

Morais, M.C., Pereira, H. 2007. Heartwood and sapwood variation in *Eucalyptus globulus labill*. Trees at the end of rotation for pulpwood production. *Annals of Forest Science*, 64: 665-671.

Nguyen, T.D., Sakakibara, K., Imai, T., Tsujii, Y., Kohdzuma, Y. and Sugiyama, J. (2018). Shrinkage and swelling behavior of archaeological waterlogged wood preserved with slightly crosslinked sodium polyacrylate. *Journal of Wood Science*, 64(3), pp.294–300.

Pagel, C. 2019, *Investigation into material resistance factors properties of young engineered Eucalyptus grandis timber*. Stellenbosch University. MSc thesis, Available [https://scholar.sun.ac.za] 16 November 2019.

Panigrahi, S., Kumar, S., Panda, S., Borkataki, S. 2018. Effect of permeability on primary processing of wood. *Journal of Pharmacognosy and Phytochemistry*, 7(4): 2593-2598.

Pillai, P.K.C., Pandalai, R.C., Dhamondaran, T.K., Sankaran, K.V. 2013, Wood density and heartwood proportion in *Eucalyptus* trees from intensively-managend short -rotation in Kerala, India. *Journal of Tropical Forest Science,* 25: 220-227.

Priadi, I.T., 2001. *A study of pre-treatment in the drying of regrowth Eucalyptus obliqua L'herit.* University of Tasmania. MEngSc.

Rezende, R.N., Lima, J.T., de Ramos e Paula, L.E., Hein, P.R.G., da Silva, J.R.M. 2018. Wood permeability in *Eucalyptus grandis* and *Eucalyptus dunnii*. *Floresta e Ambiente*: 25(1).

SANS 1707-1. 2010. Sawn *Eucalyptus* timber: Proof-graded structural timber. SABS standard division, *Pretoria*.

SANS 1707-2. 2010. Sawn *Eucalyptus* timber: Brandering and battens. SABS standard division, *Pretoria*.

SANS 1783-1. 2009. Sawn softwood timber: General requirements. SABS standard division, *Pretoria*.

SANS 1783-2. 2012. Sawn softwood timber: Stress-graded structural timber and for frame wall construction. SABS standard division, *Pretoria*.

SANS 1783-3. 2010. Sawn softwood timber: Industrial timber. SABS standard division, *Pretoria*.

SANS 1783-4. 2012. Sawn softwood timber: Brandering and battens. SABS standard division, *Pretoria*.

Sharma, S.K., Shukla, S.R., Shashikala, S. and Poornima, V.S. 2015. Axial variations in anatomical properties and basic density of Eucalypt urograndis hybrid (*Eucalyptus grandis* × *E. urophylla*) clones. *Journal of Forestry Research*, 26(3): 739–744.

Tsoumis, G. (1991). *Science and technology of wood.* First ed. Remagen-Oberwinter: Kessel.

Vermaas HF, Bariska M. 1994. Collapse during low temperature drying of Eucalyptus grandis W. Hill and Pinus silvestris L. In: *Proceedings IUFRO Wood Drying Conference, Rotorua, New Zealand*, 141–150.

Wessels, C.B., Crafford, P.L., Du Toit, B., Grahn, T., Johansson, M., Lundqvist, S.O., Säll, H. and Seifert, T. 2016. Variation in physical and mechanical properties from three drought tolerant *Eucalyptus* species grown on the dry West Coast of Southern Africa. *European Journal of Wood and Wood Products*, 74: 563-575.

Wessels, C.B., Crafford, P.L., Du Toit, B., Grahn, T., Johansson, M., Lundqvist, S.O., Säll, H. and Seifert, T. 2016. Variation in physical and mechanical properties from three drought tolerant

Eucalyptus species grown on the dry west coast of Southern Africa. European *Journal of Wood and Wood Products*, 74(4): 563–575.

Wilkins, A.P., Horne, R. 1991. Wood-density variation of young plantation-grown *Eucalyptus grandis* in response to silvicultural treatments. *Forest Ecology and Management*, 40: 39-50.

Wu, Y., Hayashi, K., Liu, Y., Cai, Y. and Sugimori, M. (2006). Relationships of anatomical characteristics versus shrinkage and collapse properties in plantation-grown eucalypt wood from China. *Journal of Wood Science*, 52(3): 187-194.

Wu, Y., Hayashi, K., Liu, Y., Cai, Y., Sugimori, M. and Luo, J. 2005. Collapse-type shrinkage characteristics in plantation-grown *Eucalyptus*: I. Correlation of basic density and some structural indices with shrinkage and collapse properties. *Journal of Forestry Research*, 16(2): 83-88.

Yamashita, K., Hirakawa, Y., Nkatani, H., Ikeda, M., 2009. Longitudinal shrinkage variations within trees of sugi (Cryptomeria japonica) cultivars. *Journal of Wood Science*, 55: 1-7.

Yamashita, K., Hirakawa, Y., Nkatani, H., Ikeda, M., 2009. Tangential and radial shrinkage variation within trees of sugi (*Cryptomeria japonica*) cultivars. *Journal in Wood Science*, 55: 161-168.

Yang JL, Evans R. 2003. Prediction of MOE of eucalypt wood from microfibril angle and density. *Holz Roh Werkst* 61(6):449–452.

Yang, J.L., Ilic, J., Evans, R. 2003. Interrelationships between shrinkage properties, microfibril angle, and cellulose crystallite width in 10-year-old *Eucalyptus globulus*. *New Zealand Journal of Forestry Science*, 33(1): 47-61.

Yang, L., Liu, H. 2018. A review of Eucalyptus wood collapse and its control during drying. *BioResourves*. 13(1): 2171-2181.

Zanuncio, A.J.V., Carvalho, A.G., da Silva, L.F., Lima, J.T., Trugilho, P.F., da Silva, J.R.M. 2015. Predicting moisture content from basic density and *Eucalyptus* and *Corymbia* logs. *Ciencia y tecnología*, 17(2): 335 – 344.

Appendix A

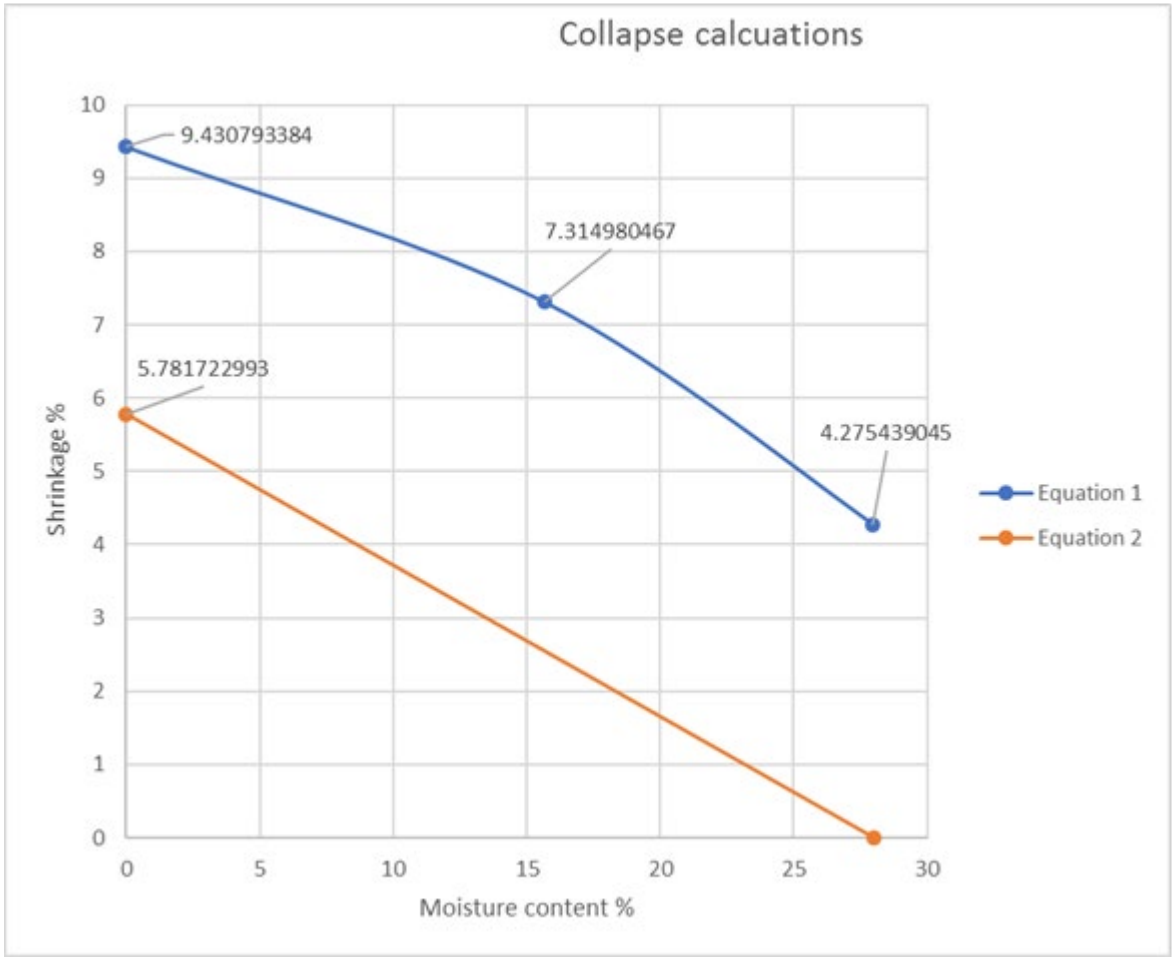

Figure A- 1*:* The calculate of collapse and shrinkage were calculated using the curves. Equations are as explained in section 3.2.1